From Telescopes to Colliders: Probing Axion-Like Particles

Yan Luo

December 2, 2024

Introduction

- Current status of ALP detection

C. O'Hare. https://cajohare.github.io/AxionLimits/

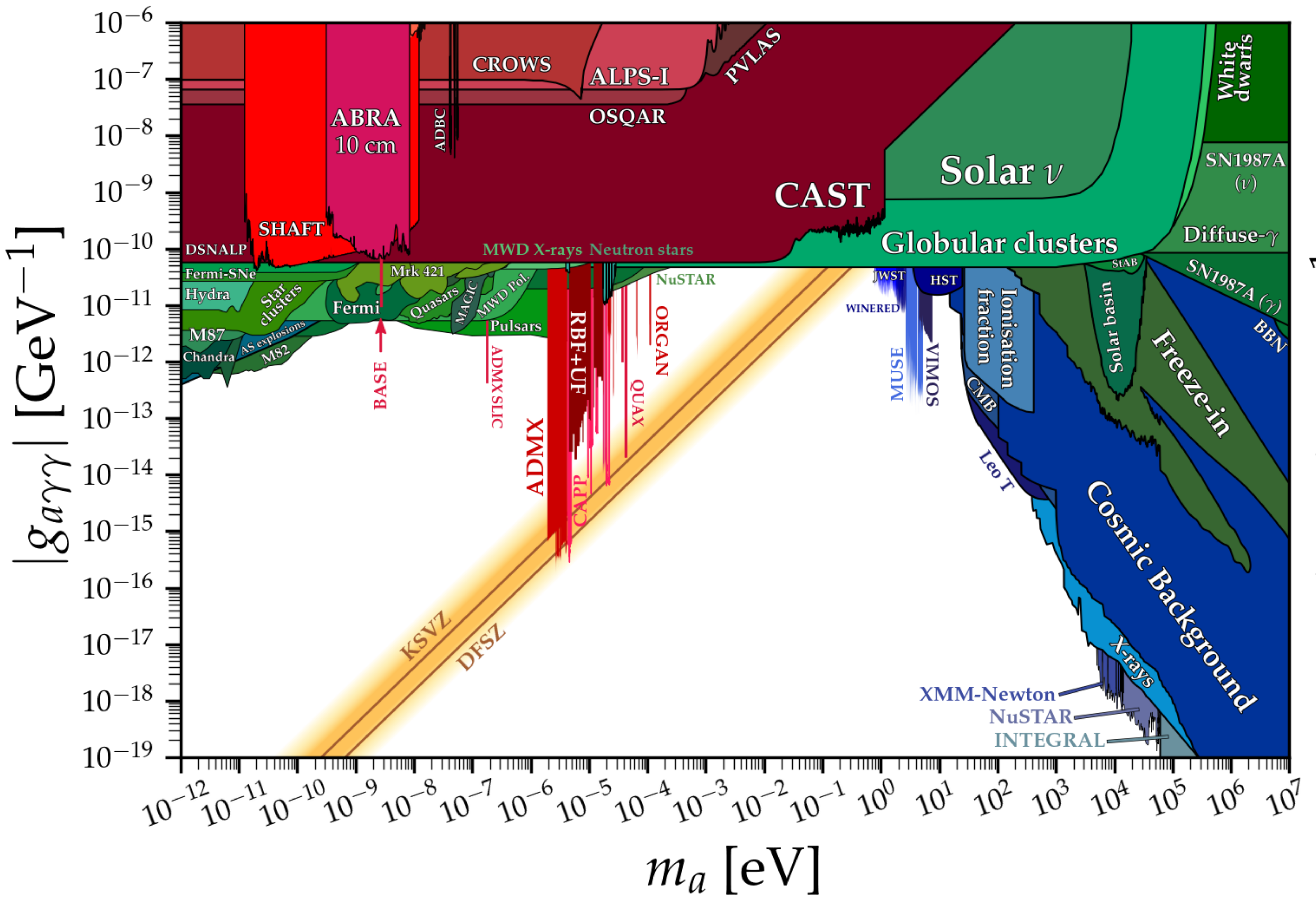

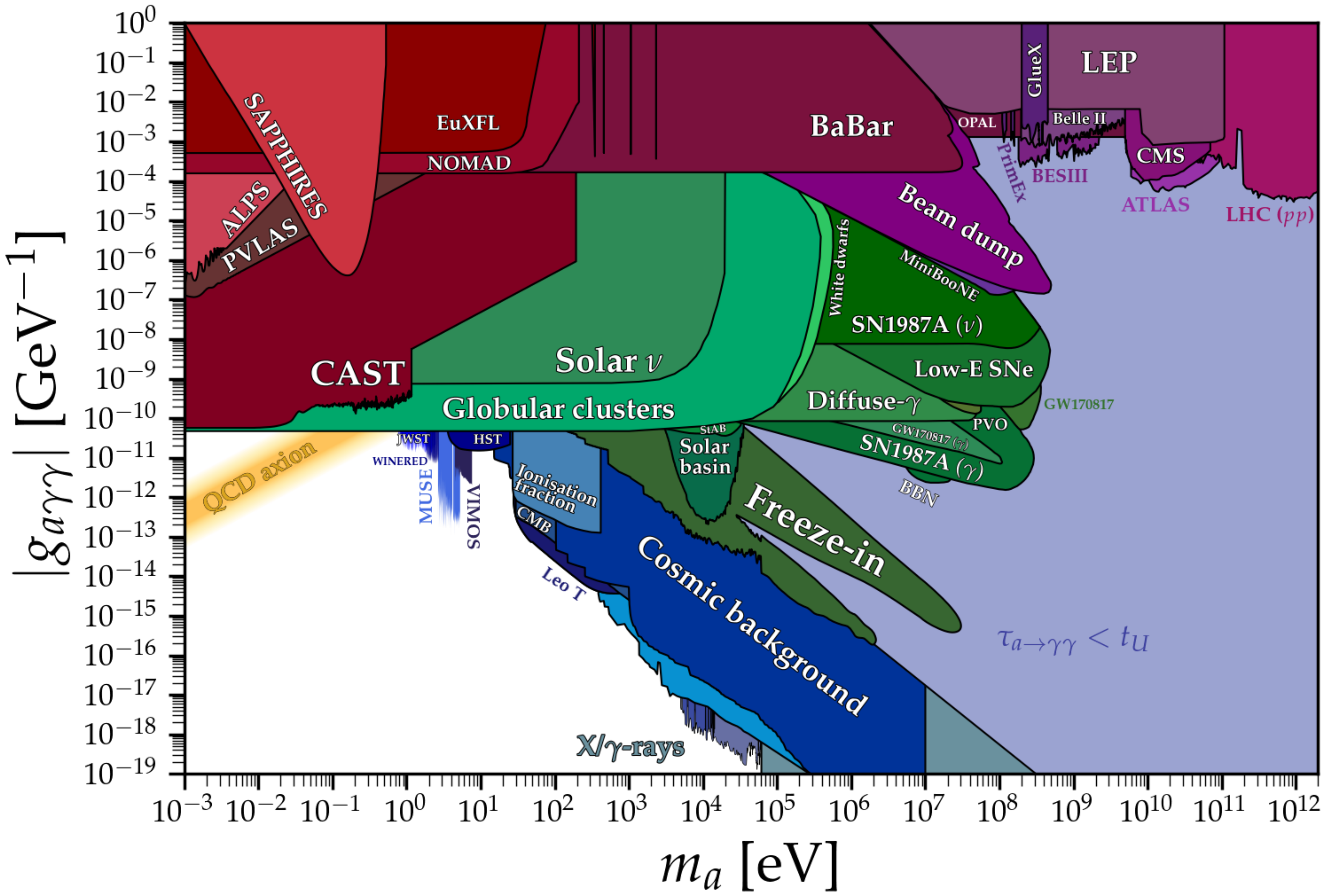

Yan Luo

Introduction

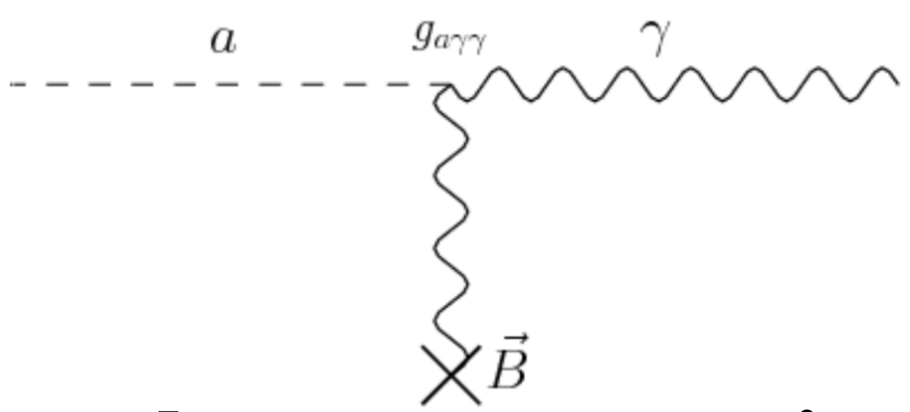

- Ultralight ALP search strategy

C. O'Hare. https://cajohare.github.io/AxionLimits/

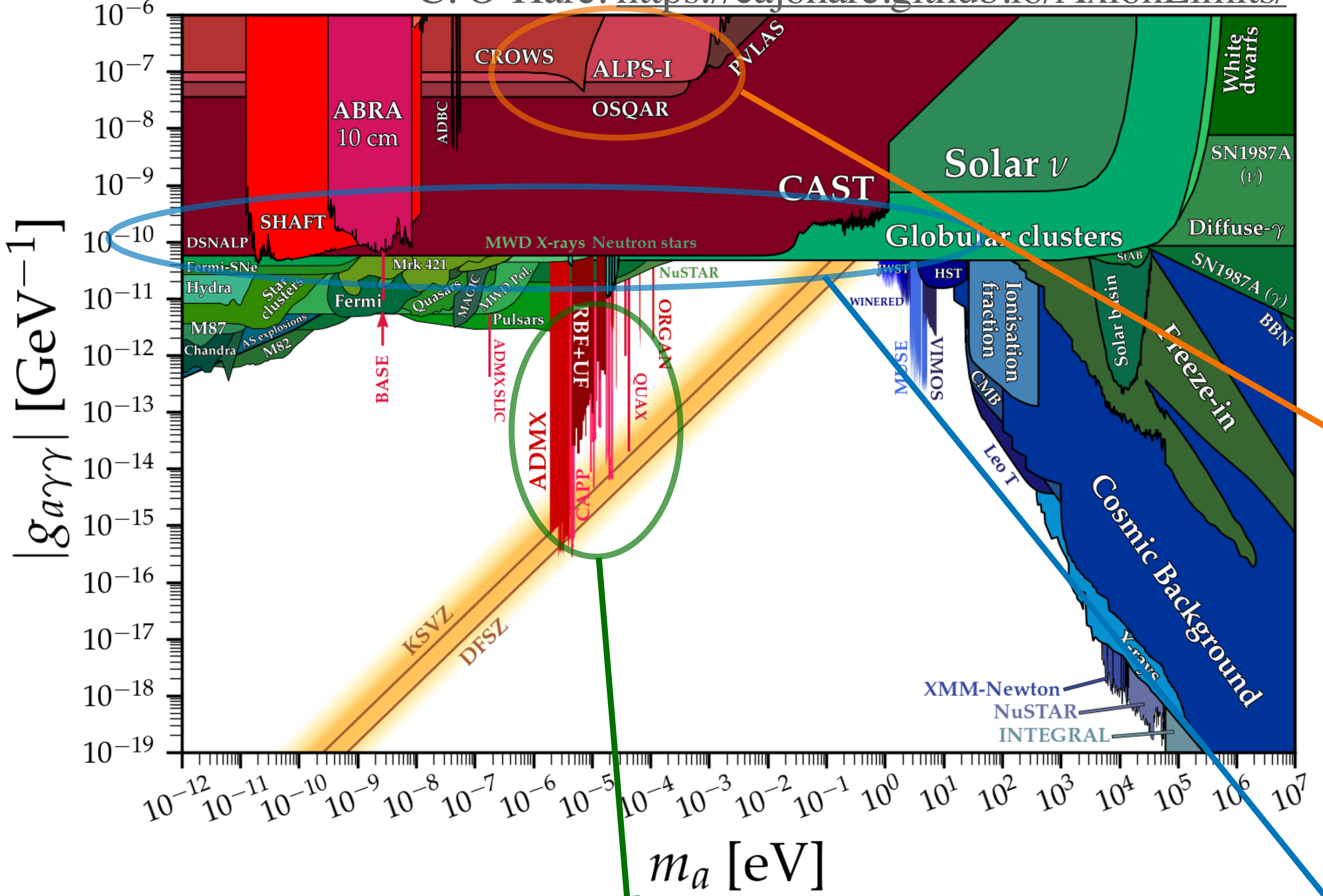

the main search strategy: **axion-photon conversion**

$$\mathscr{L}_{a\gamma} = \frac{1}{2}\partial_\mu a \partial^\mu a - \frac{1}{2}m_a^2 a^2 + \frac{1}{4}g_{a\gamma\gamma} a F_{\mu\nu}\tilde{F}^{\mu\nu}$$

magnetic field background $-g_{a\gamma\gamma} a \mathbf{B_0} \cdot \mathbf{E}$

can be ultralight dark matter

dark photon also share the similar phenomenology

R. Battesti et al. 1803.07547

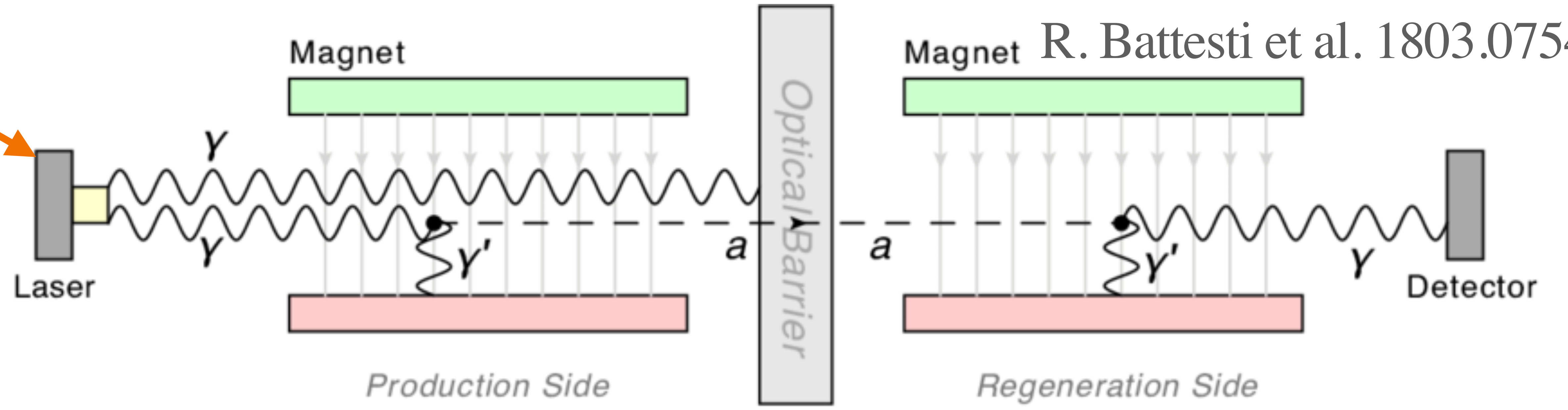

light-shining-through-walls

CAST Collaboration. 1705.02290

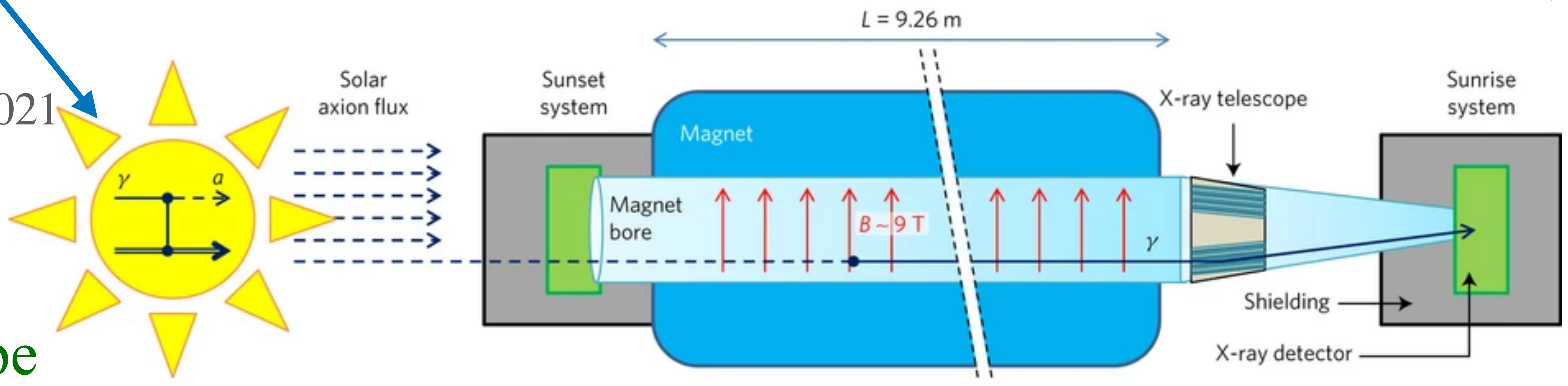

helioscope: CAST

I. G. Irastorza, Nature News & views 2021

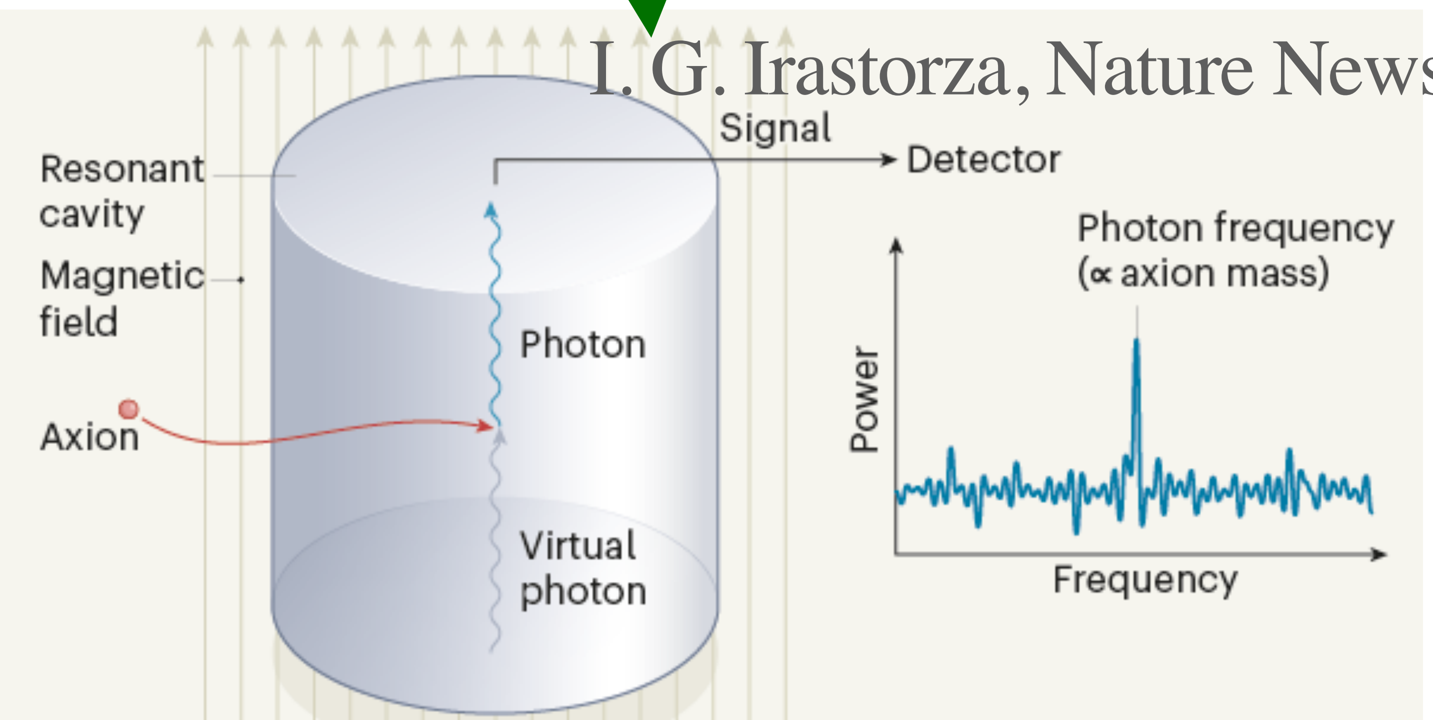

haloscope

cavity

Yan Luo

Introduction

David McKeen et al. 1609.06781

- Searches for heavier ALP MeV - GeV

collider searches, beam dump searches

beam dump: high luminosity, can probe smaller coupling

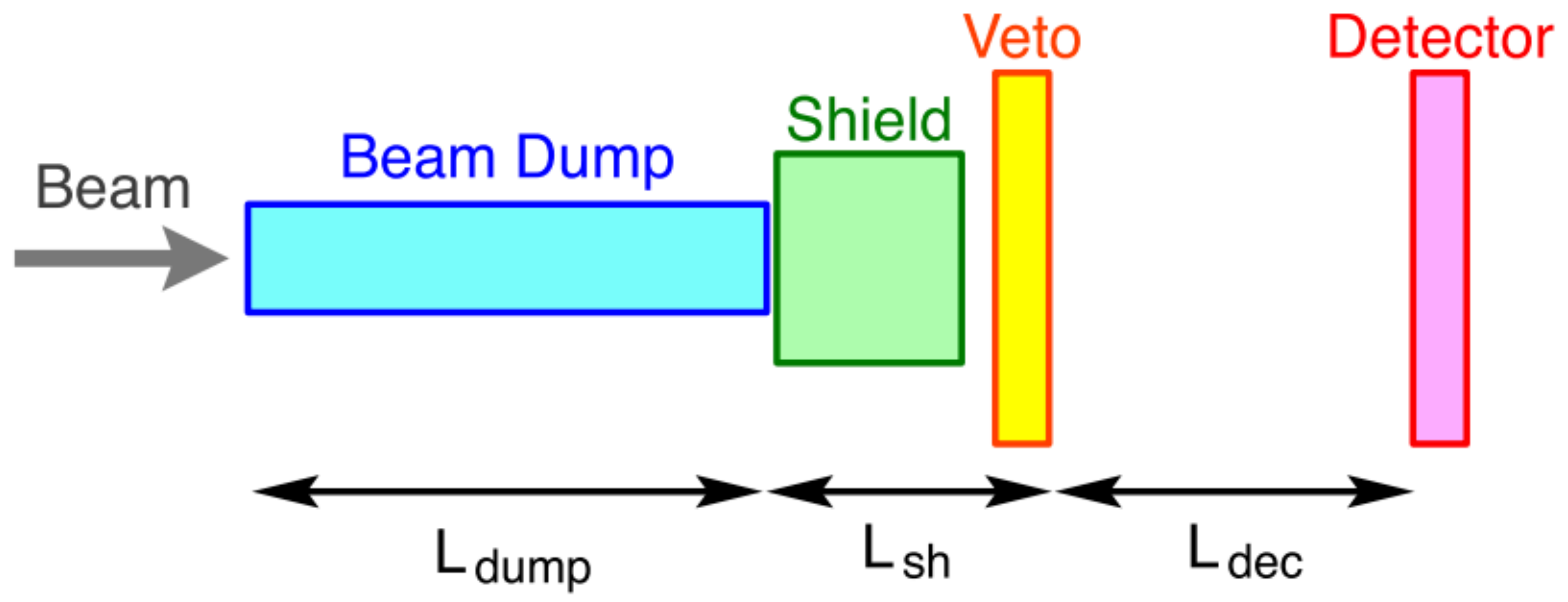

M. Bauer et al. 1708.00443

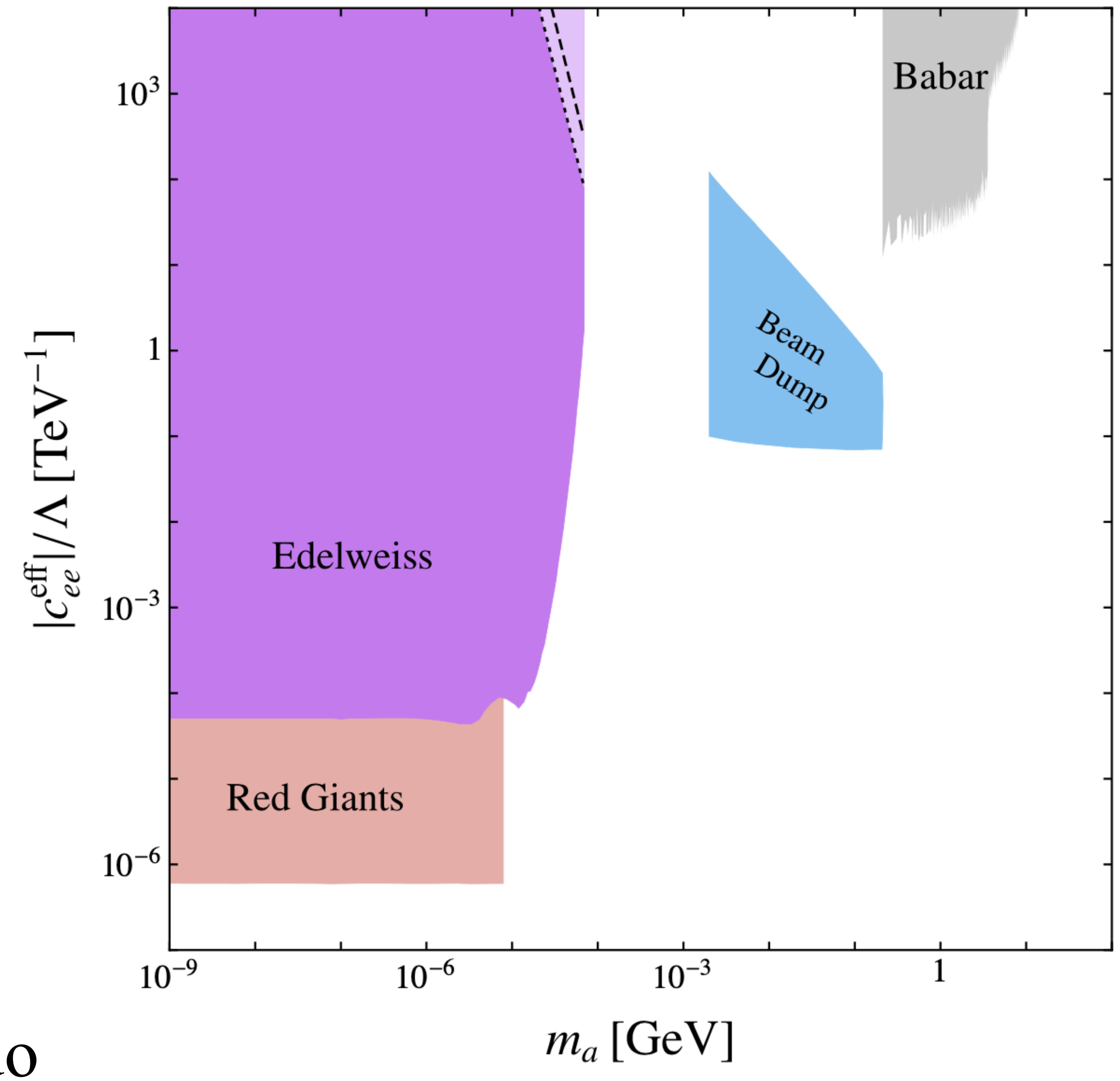

BESIII Collaboration et al. 2211.12699

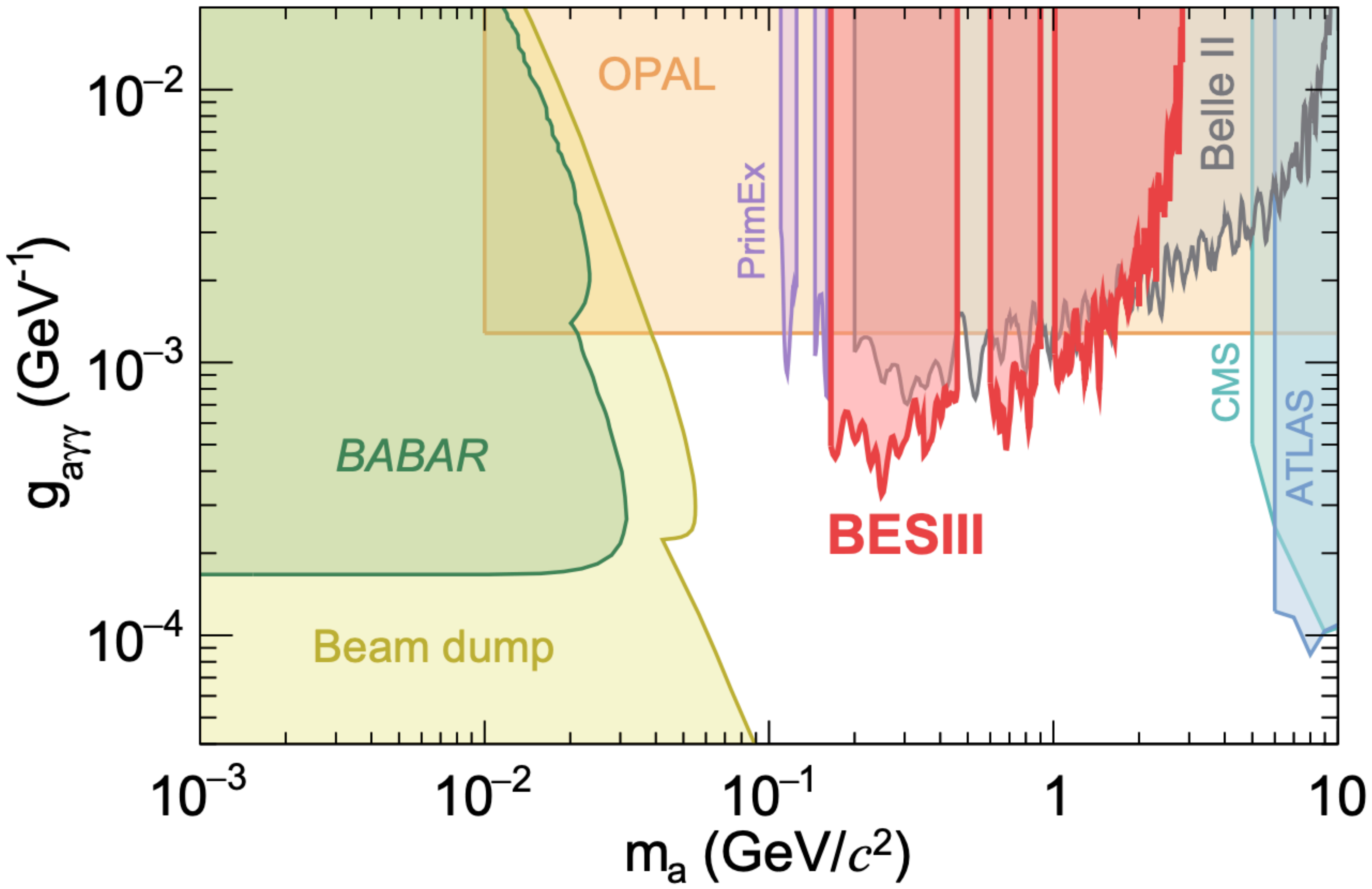

Yan Luo

- Searching for Ultralight Dark Matter Conversion in Solar Corona using LOFAR Data [arXiv: 2301.03622]

- Investigation of the concurrent effects of ALP-photon and ALP-electron couplings in Collider and Beam Dump Searches [arXiv: 2304.05435]

Resonant Conversion

$$\mathscr{L}_{a\gamma} = \frac{1}{2}\partial_\mu a \partial^\mu a - \frac{1}{2} m_a^2 a^2 - g_{a\gamma\gamma} a \mathbf{B_0} \cdot \mathbf{E}$$

photon effective mass in plasma

$$\omega_p = \left(\frac{4\pi\alpha n_e}{m_e}\right)^{1/2} = \left(\frac{n_e}{7.3\times 10^8\ \mathrm{cm}^{-3}}\right)^{1/2} \mu\mathrm{eV}$$

when $\omega_p \approx m_a$, axions can resonantly convert into photons

- Solar model

H. An, X. Chen, S. Ge, J. Liu and **YL**. 2301.03622

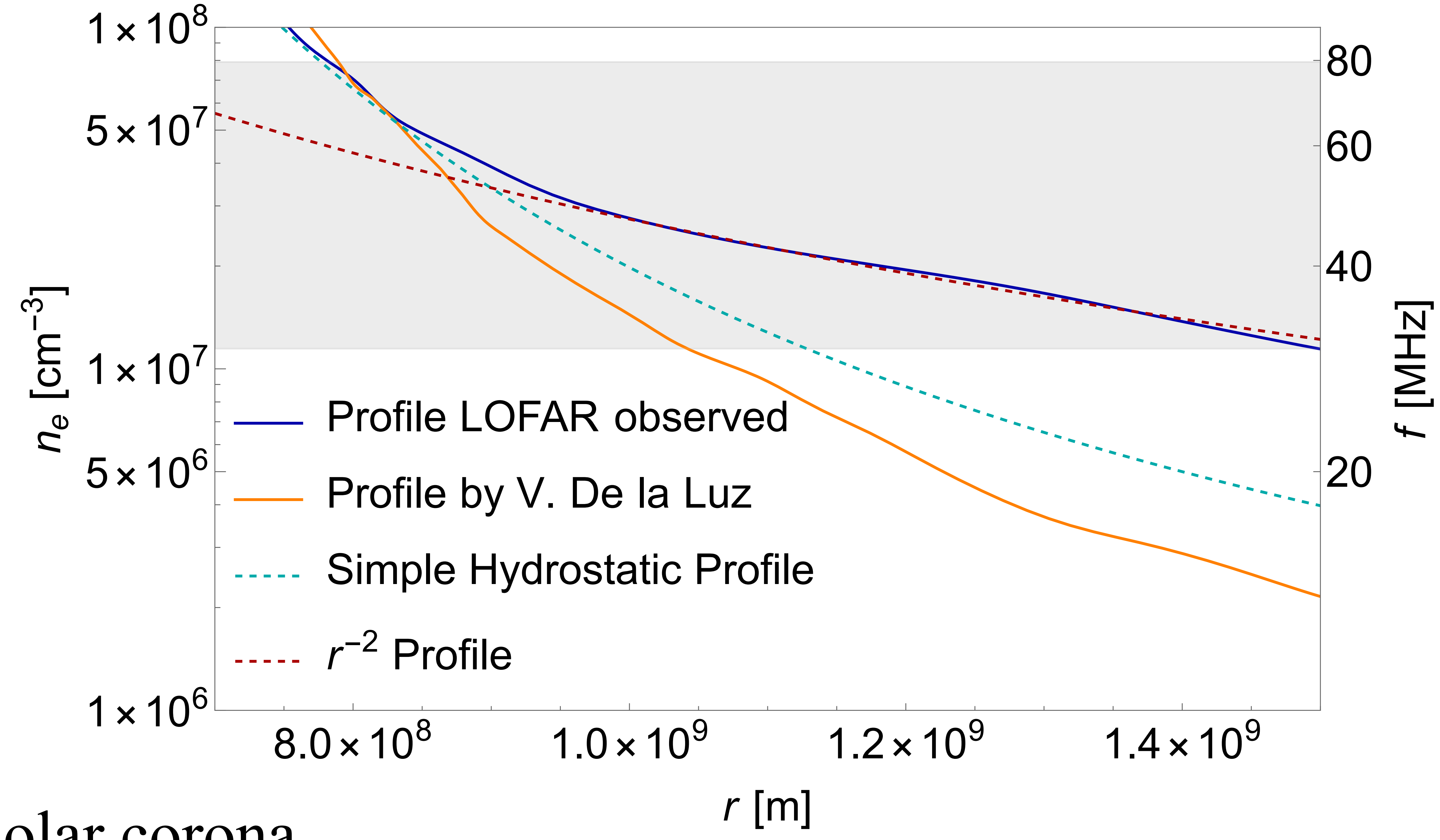

- Our neighbor: the Sun

axion DM

resonantly converts to radio-frequency EM waves in the solar corona

corresponds to $m_a \sim 10^{-7}$eV

Yan Luo

LOFAR Telescope

van Haarlem et al. 1305.3550

K. Gert et al. *Experimental Astronomy*, 56(2), pp.687-714

LOFAR: Low Frequency Array telescope

High-sensitivity interferometer

mainly in Netherland, stations

solar observation

radio frequency range:

LBA: 10 – 80 MHz

HBA: 110 – 240 MHz

Yan Luo

Conversion Probability

- Coupled equation of motion

$$\left[\frac{\partial^2}{\partial t^2} - \frac{\partial^2}{\partial r^2} + \begin{pmatrix} \omega_p^2 & -g_{a\gamma\gamma}|\mathbf{B}_T|\omega \\ -g_{a\gamma\gamma}|\mathbf{B}_T|\omega & m_a^2 \end{pmatrix}\right] \begin{pmatrix} A_{//}(r,t) \\ a(r,t) \end{pmatrix} = 0$$

treat it as classical wave

WKB approximation to 1st order PDEs

$$A(r,t) = \tilde{A}(r)\exp(-i\omega t + ik_r r)$$

$$\partial_t^2 - \partial_r^2 = -\omega^2 - \partial_r^2 \approx -2k_r(k_r + i\partial_r) - m_a^2 - k_T^2$$

- Conversion Probability

solved perturbatively

$$P_{a\to\gamma} = \left| \int_{r_0}^{r} dr' \frac{-\epsilon m_a^2}{2k_r} e^{i\int_{r_0}^{r'} dr'' \frac{1}{2k_r}\left[\omega_p(r'')^2 - m_a^2\right]} \right|^2 .$$

by saddle point approximation

$$P_{a\to\gamma}(v_{rc}) = \pi \frac{g_{a\gamma\gamma}^2 \left|\mathbf{B}_T\right|^2}{m_a} v_{rc}^{-1} \left| \frac{\partial \ln \omega_p^2(r)}{\partial r} \right|_{r=r_c}^{-1}$$

- Radiation power

considering gravitational focusing

$$\frac{d\mathscr{P}}{d\Omega} = \int d\mathbf{v}_0 f_{\mathrm{DM}}(\mathbf{v}_0) P_{A'\to\gamma}(v_0)\rho_{\mathrm{DM}} v(r_c) r_c^2$$

$$v(r_c) = \sqrt{v_0^2 + 2G_N M_\odot / r_c}$$

Yan Luo

Propagation in Solar Plasma

- Spectral flux density

$$S_{\rm sig} = \frac{1}{\mathscr{B}} \frac{1}{d^2} \frac{d\mathscr{P}}{d\Omega} P_{\rm sur}(f)\beta(f)$$

bandwidth $\mathscr{B} = 97$ kHz

$P_{\rm sur}(f), \beta(f)$ are the suppresion factors due to propagation effect

- Smearing

naively speaking, the direction of the outgoing photon from plasma is determined by the rule of refraction

$$\frac{n(r_c)}{n(r)} = \frac{\sin\theta(r)}{\sin\theta(r_c)} \qquad n(r) = \frac{k}{\omega} = \sqrt{1 - \frac{\omega_p^2(r)}{\omega^2}}$$

at the position of resonance: $n(r_c) \sim v \sim 10^{-3}$ θ quickly goes to 0

however, considering the scattering in the inhomogenous plasma, the outgoing angular distribution will be broadened: **smearing effect**

field of view $\sim 10^{-3}$

- Absorption

mainly through inverse bremsstrahlung, depends on the path

$P_{\rm sur}(f)$

Yan Luo

Propagation in Solar Plasma

- MC ray-tracing simulation

P. Kontar et al. 1909.00340

Applying the ray-tracing numerical code from P. Kontar et al. 2019
to calculate these suppression factors
based on the Fokker-Planck equation:
describing the evolution of phase-space distribution $N(\mathbf{r}, \mathbf{k}, t)$ of photons

$$\beta(f) = \frac{d^2}{R_S^2} \int_{\text{beam}} \frac{g(\theta_1, \phi_1)}{r^2} dS$$

$g(\theta_1, \phi_1)$ angular distribution at R_S

H. An, X. Chen, S. Ge, J. Liu and **YL**. 2301.03622

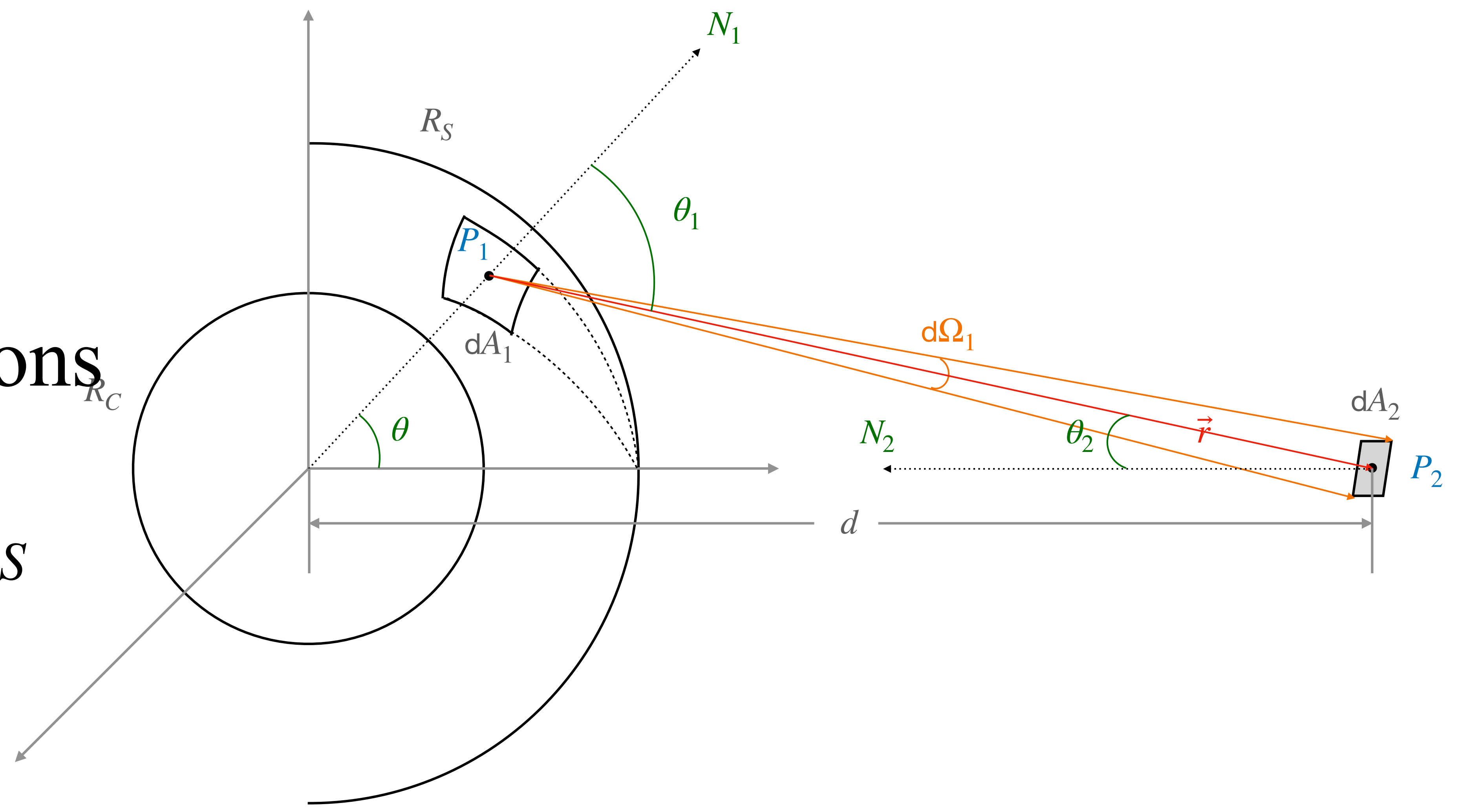

H. An, X. Chen, S. Ge, J. Liu and **YL**. 2301.03622

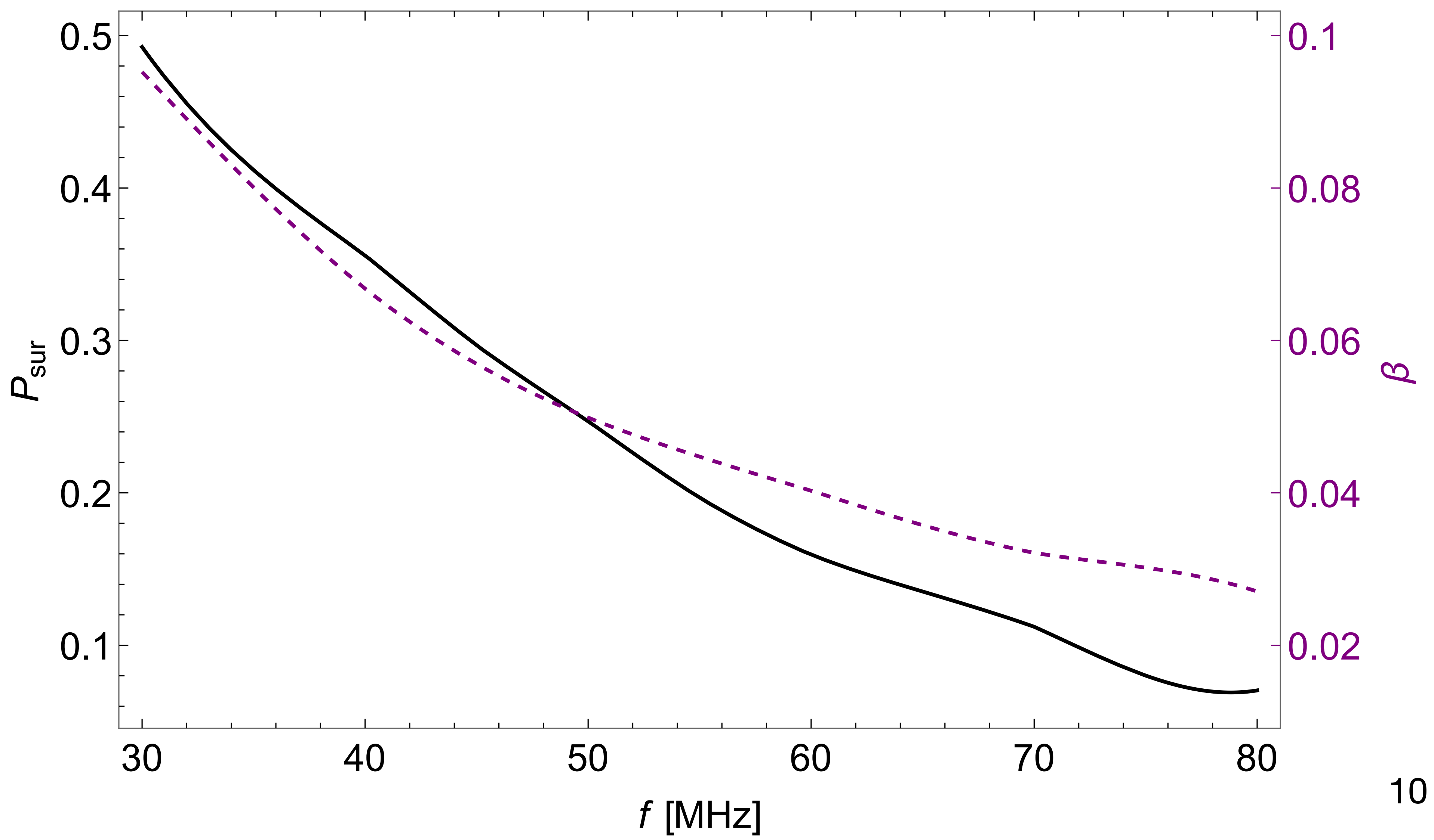

small field of view (FOV)

$$\text{FWHM} = \eta \times \frac{\lambda}{D} \sim 10^{-3}\ \text{rad} \qquad \eta = 1.02,\ D \sim 3.5\ \text{km}$$

decreasing smearing factor mainly
comes from decreasing FOV for higher frequency

Yan Luo

Data Analysis

- LOFAR data

frequency range: 30 - 80MHz

divided the time bins into 150 intervals

do **data cleaning** for time bins to remove transient noises:

$$\mu_t[\text{test}] < \mu_t[\text{ref}] + 2\sigma_t[\text{ref}]$$

$$\sigma_t[\text{test}] < 2\sigma_t[\text{ref}]$$

- Log-likelihood ratio test

likelihood function:

$$B(a, f_i) = \Sigma_{j=0}^{3} a_j f_i^j$$

$$L(S, a) = \prod_{i=i_0-5}^{i_0+5} \frac{1}{\sigma_i \sqrt{2\pi}} \exp\left[-\frac{1}{2} \left(\frac{B(a, f_i) + S\delta_{ii_0} - \bar{O}_i}{\sigma_i} \right)^2 \right]$$

test statistic $q_S = \begin{cases} -2\ln\left[\frac{L(S,\tilde{a})}{L(\hat{S},\hat{a})}\right], & \hat{S} \le S \\ 0, & \hat{S} > S \end{cases}$ half-χ^2 asymptotic

$$h(q_S \mid S) = \frac{1}{2}\delta(q_S) + \frac{1}{2}\frac{1}{\sqrt{2\pi}}\frac{1}{\sqrt{q_S}} e^{-q_S/2}$$

H. An, X. Chen, S. Ge, J. Liu and **YL**. 2301.03622

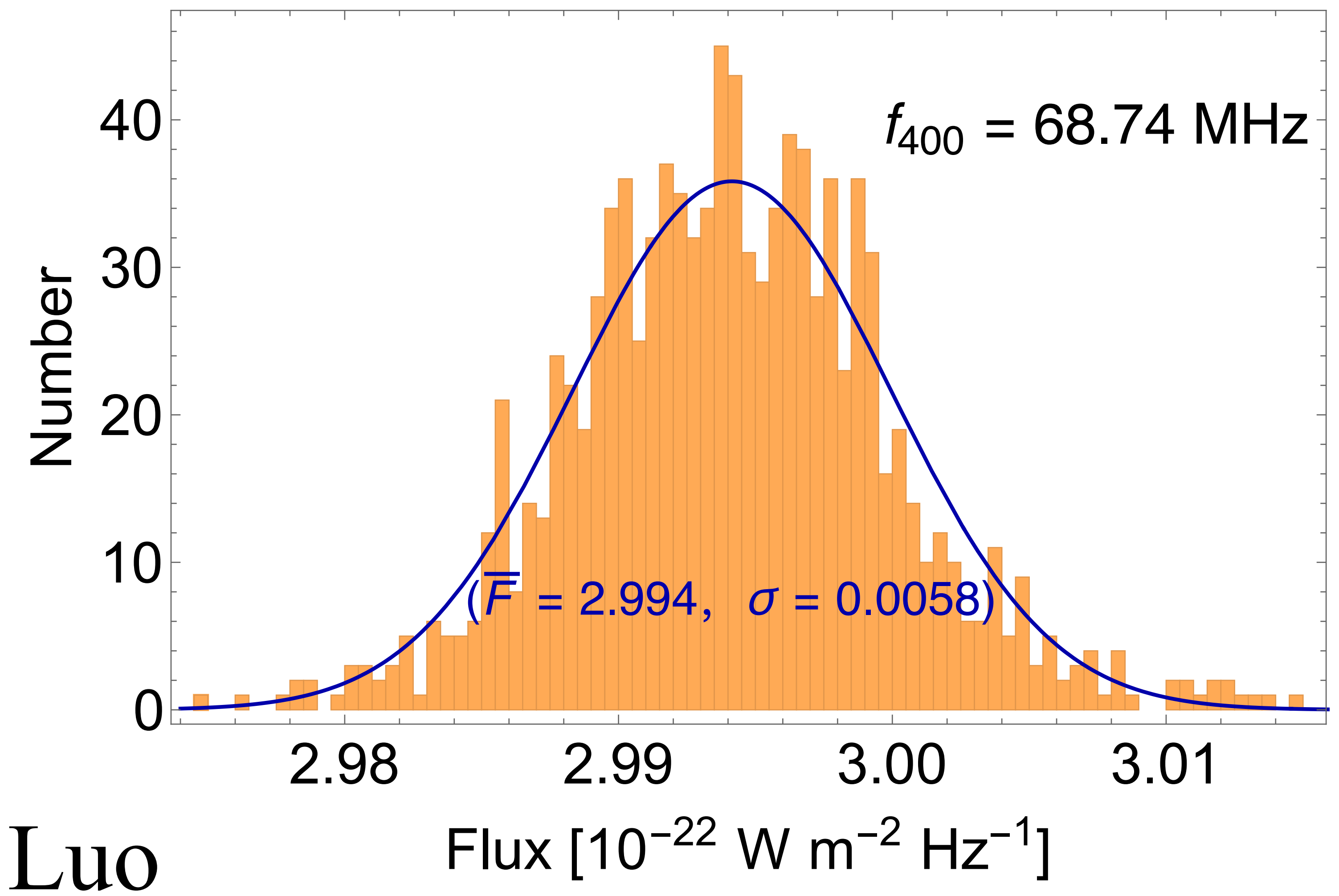

Model-independent 95% C.L. upper limits from LOFAR data

H. An, X. Chen, S. Ge, J. Liu and **YL**. 2301.03622

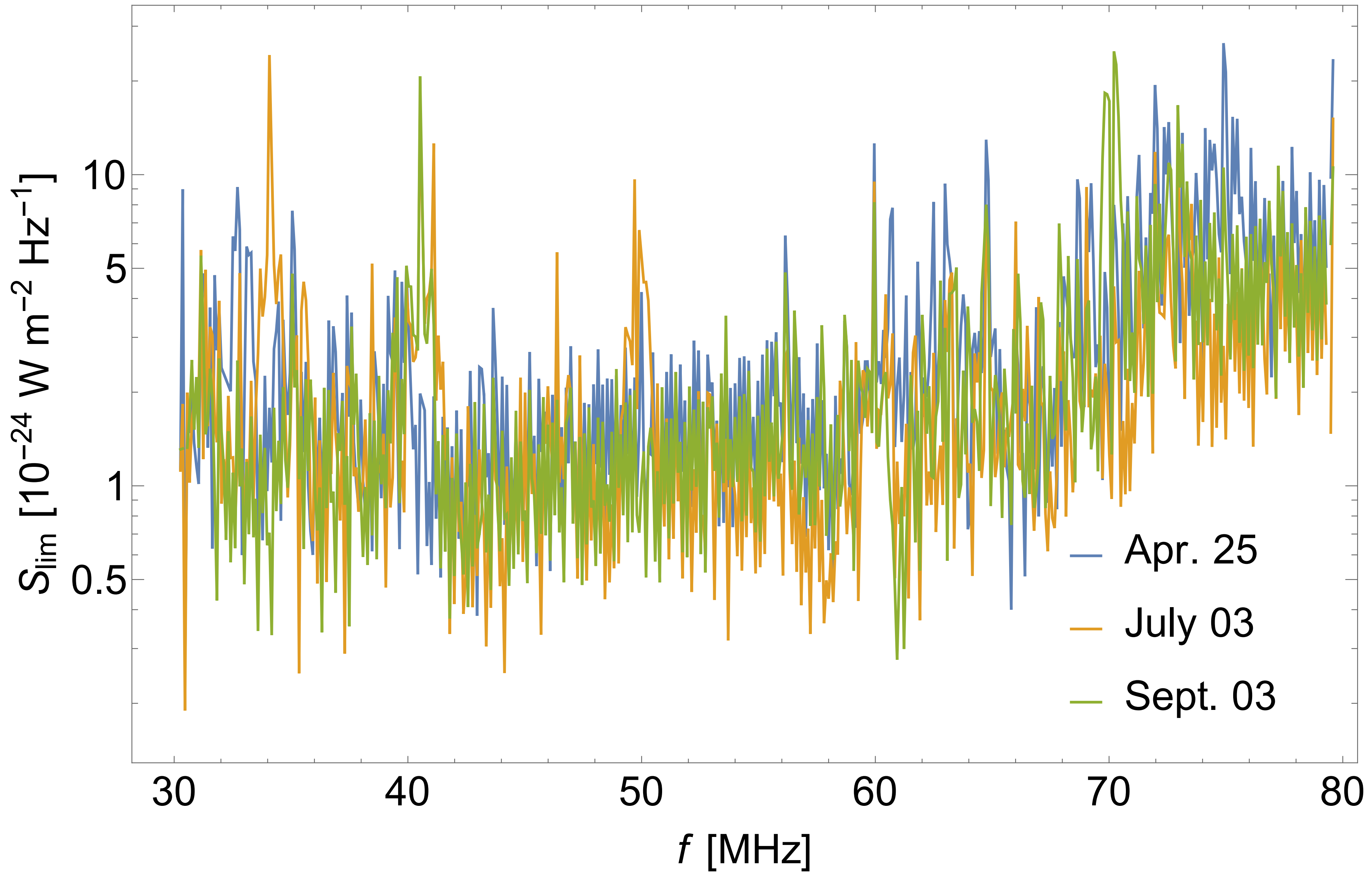

Results

- magnetic field profile:

  dipole-like magnetic field,
  but large fluctuation

  $$\left|\mathbf{B}_T\right| \sim 1 \text{ Gauss at } 1.05R_\odot$$

  Z. Yang et al. 2008.03136

  $$r_c \sim 2.18 - 1.12R_\odot \text{ for } 30 - 80 \text{ MHz}$$

  following R^{-3} decreasing

- better than the constraints from Light-Shining-through-a-Wall experiments but does not exceed the CAST or other astrophysical bounds

H. An, X. Chen, S. Ge, J. Liu and **YL**. 2301.03622

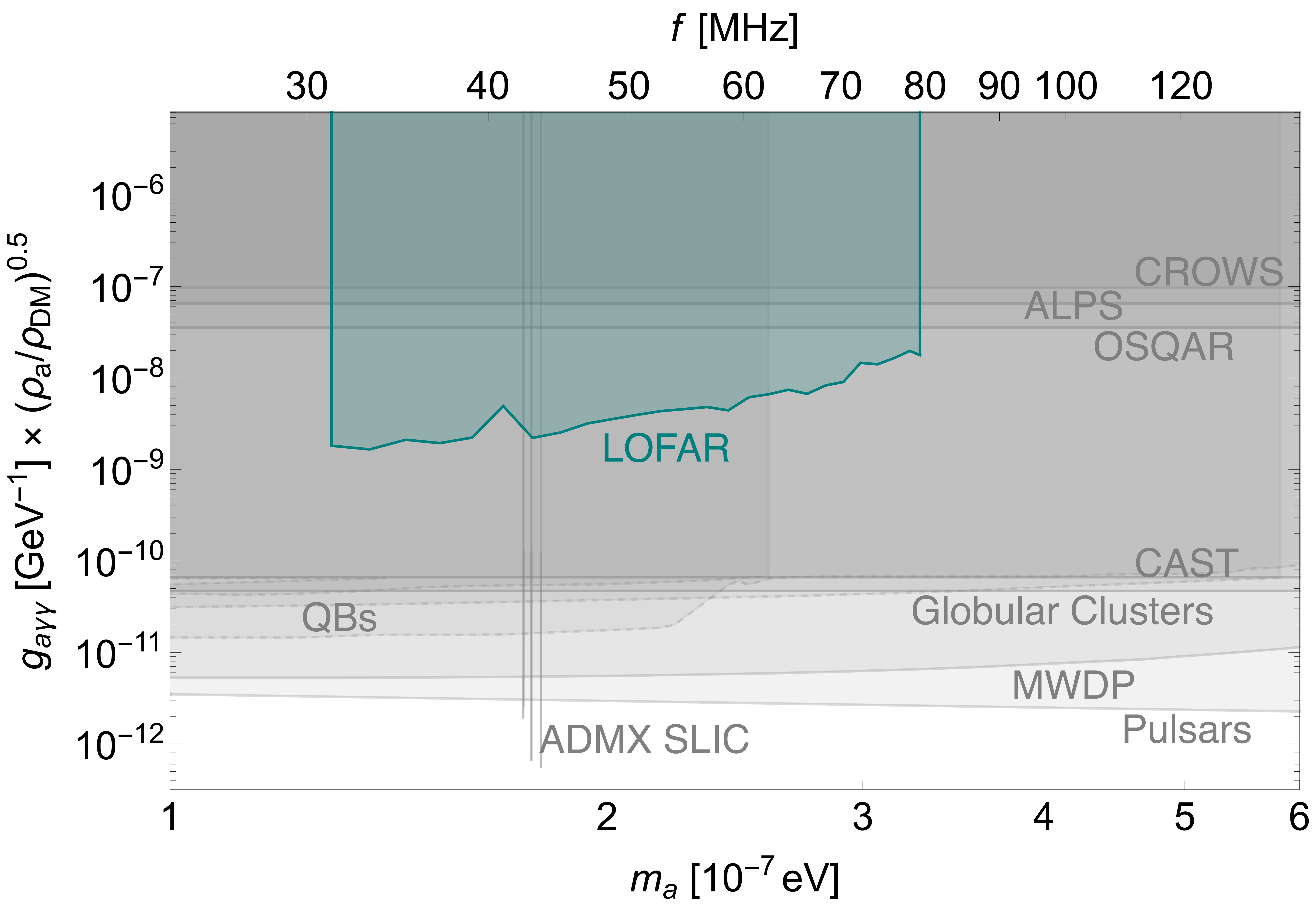

Large magnetic field uncertainty, overshadow the uncertainty of data.
Average over 20 frequency bins.

Yan Luo

Dark Photon Case

A. Caputo et al. 2105.04565

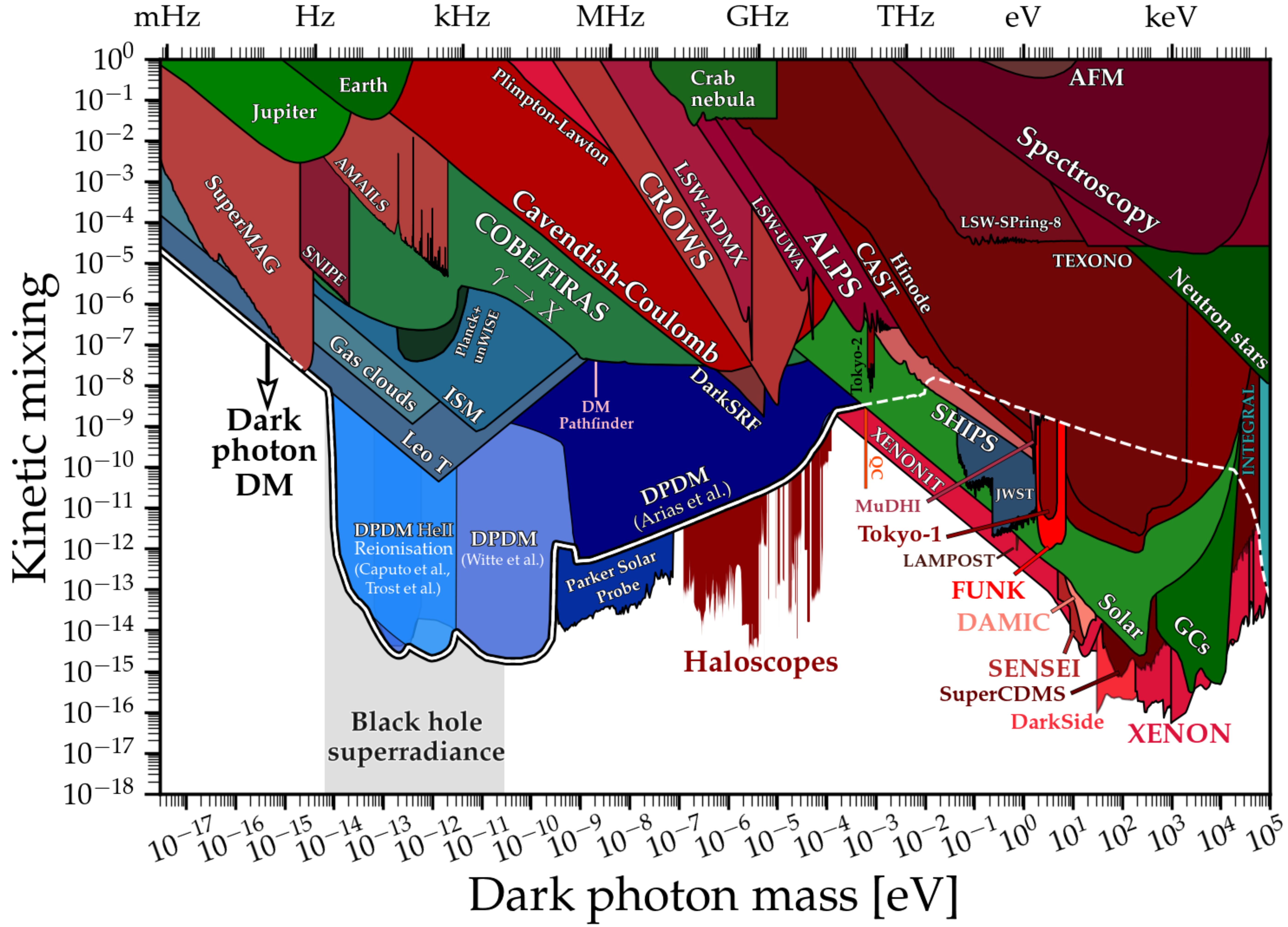

$$\mathscr{L}_{A'\gamma} = -\frac{1}{4}F'_{\mu\nu}F'^{\mu\nu} + \frac{1}{2}m_{A'}^2 A'_\mu A'^\mu - \frac{1}{2}\epsilon F_{\mu\nu}F'^{\mu\nu}$$

$$\left[\frac{\partial^2}{\partial t^2} - \frac{\partial^2}{\partial r^2} + \begin{pmatrix} \omega_p^2 & -\epsilon m_{A'}^2 \\ -\epsilon m_{A'}^2 & m_{A'}^2 \end{pmatrix}\right] \begin{pmatrix} A(r,t) \\ A'(r,t) \end{pmatrix} = 0$$

$m_{A'}$: DPDM mass

ϵ: kinetic mixing parameter

$$P_{A'\to\gamma}(v_{rc}) = \frac{2}{3} \times \pi\epsilon^2 m_{A'} v_{rc}^{-1} \left|\frac{\partial \ln \omega_p^2(r)}{\partial r}\right|^{-1}_{r=r_c}$$

Yan Luo

Dark Photon Case

- the upper limit on ϵ is about 10^{-13} in the frequency range 30-80 MHz

- about one order of magnitude better than the existing CMB constraint

- complementary to other searches for DPDM with higher frequency, such as the Dark E-field experiment

H. An, X. Chen, S. Ge, J. Liu and **YL**. 2301.03622

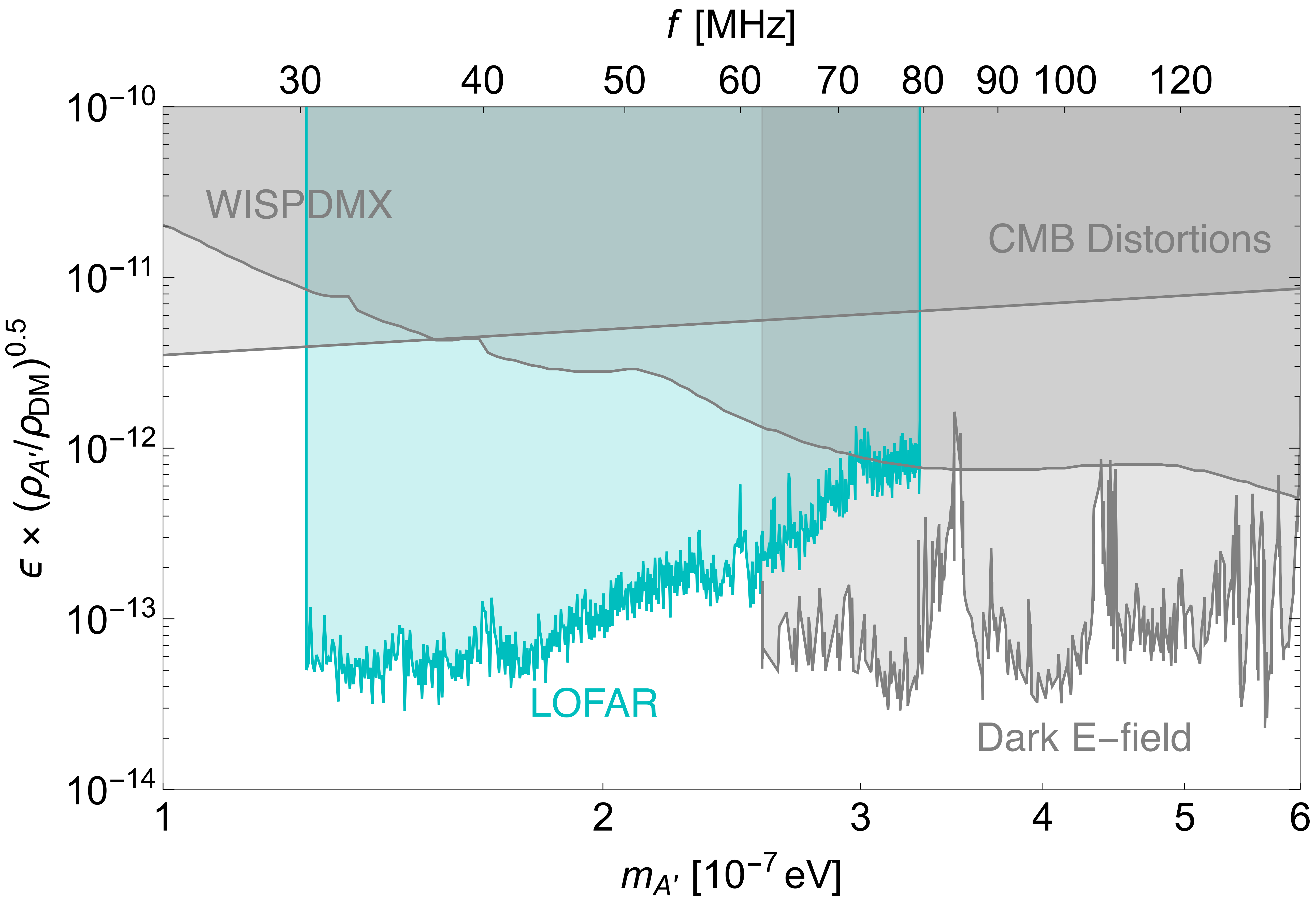

Yan Luo

- Searching for Ultralight Dark Matter Conversion in Solar Corona using LOFAR Data [arXiv: 2301.03622]

- Investigation of the concurrent effects of ALP-photon and ALP-electron couplings in Collider and Beam Dump Searches [arXiv: 2304.05435]

Introduction

• ALP Searches

- previous study: seperately consider the ALP interactions with fermions and gauge bosons
- concurrence of ALP couplings naturally arises from UV models, and loop corrections
- We investigate the concurrence effect of ALP-γ and ALP-e couplings in e^-e^+ colliders and beam dump experiments

M. Bauer et al. 1708.00443

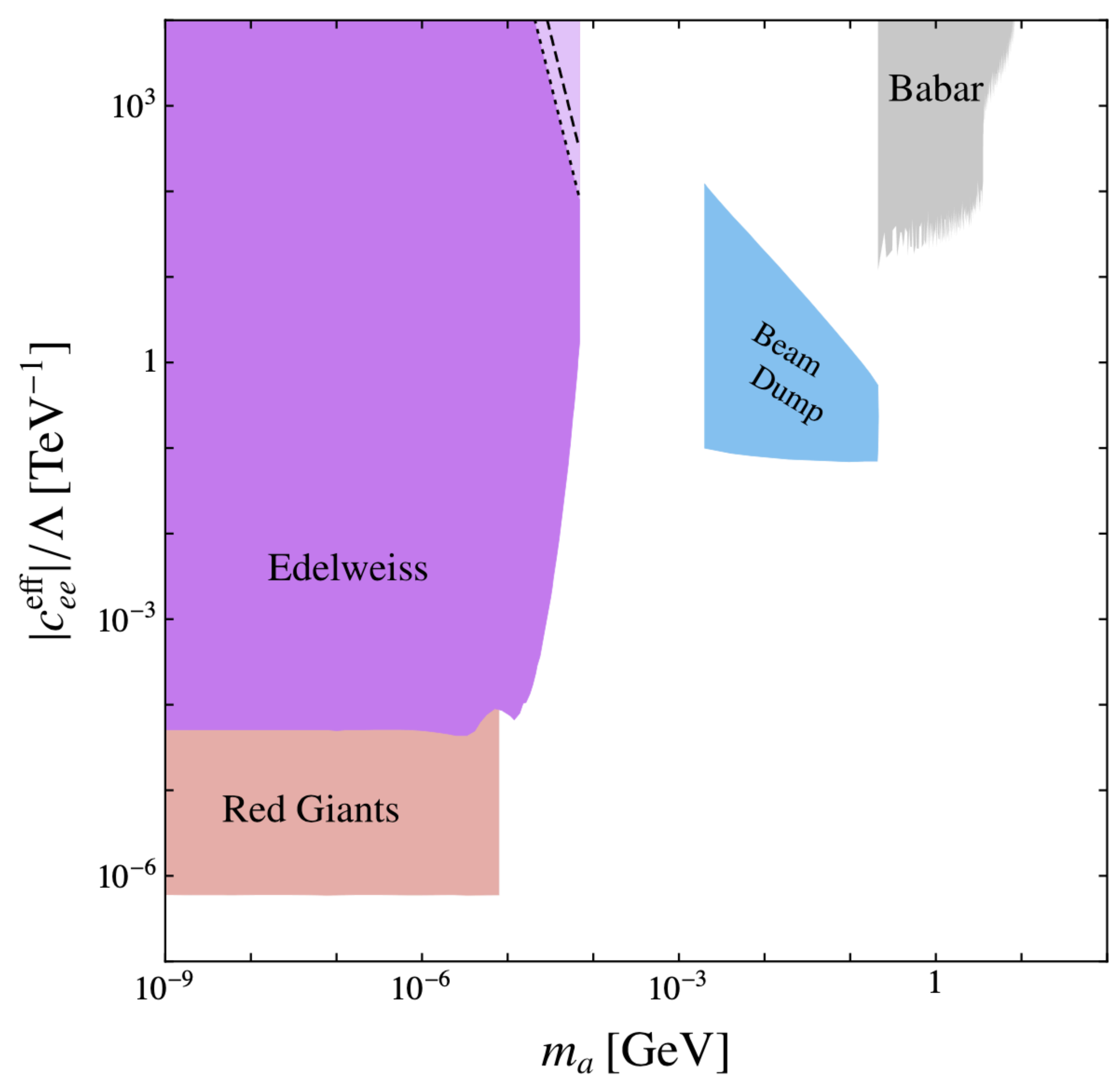

Belle II Collaboration. 2007.13071

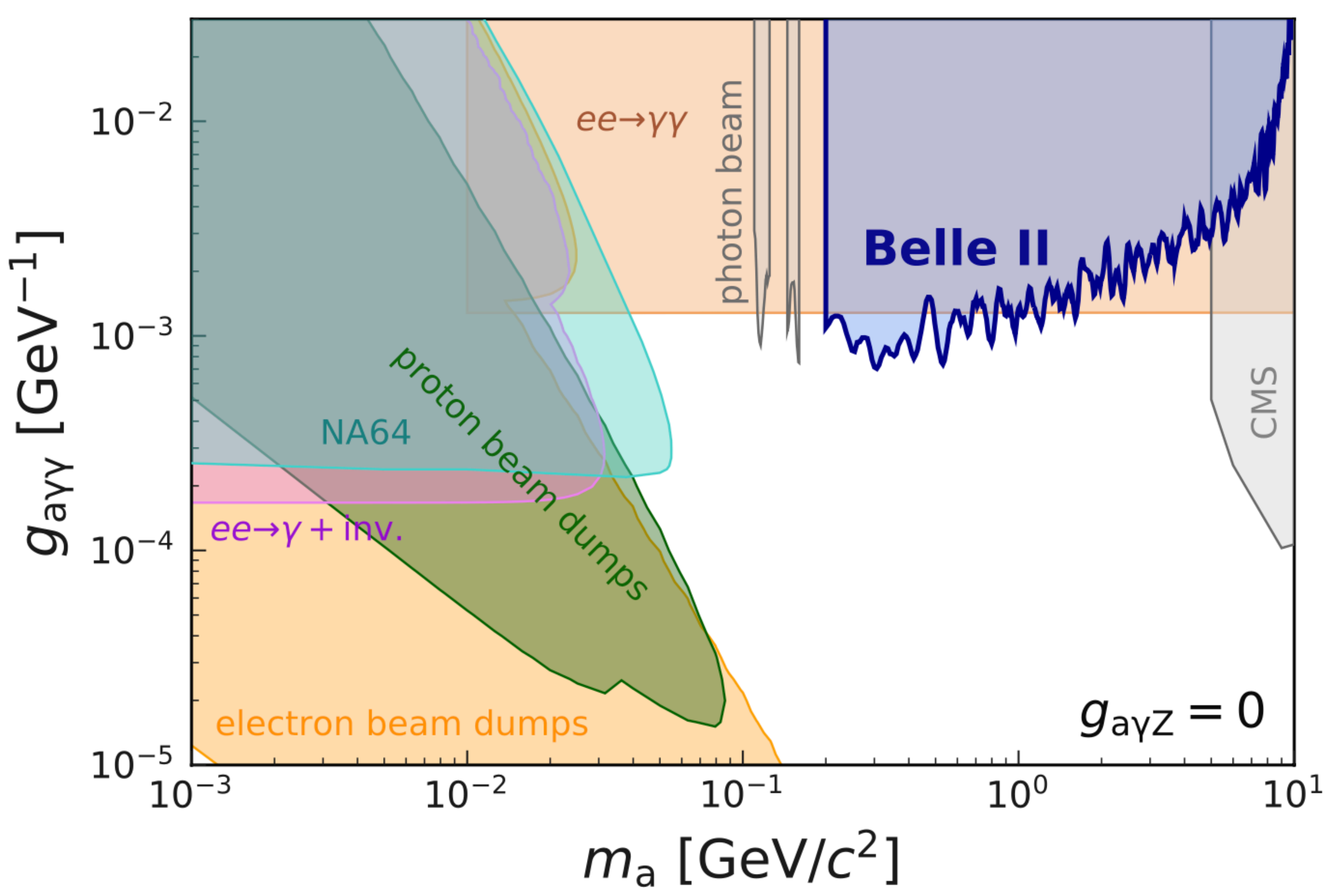

Yan Luo

Simplified Model

- Effective Lagrangian

$$\mathscr{L}_{ALP} = \frac{1}{2}\partial_\mu a \partial^\mu a - \frac{1}{2} m_a^2 a^2 + \frac{1}{2} g_{aee}^{\text{eff}} \partial_\mu a \bar{e} \gamma^\mu \gamma_5 e - \frac{1}{4} g_{a\gamma\gamma}^{\text{eff}} a F_{\mu\nu} \tilde{F}^{\mu\nu}$$

- Decay

$$\Gamma_{a \to e\bar{e}} = \frac{(g_{a\bar{e}e}^{\text{eff}})^2 m_e^2 m_a}{8\pi} \left(1 - \frac{4m_e^2}{m_a^2}\right)^{\frac{1}{2}}$$

$$\Gamma_{a \to \gamma\gamma} = \frac{(g_{a\gamma\gamma}^{\text{eff}})^2 m_a^3}{64\pi}$$

$$\frac{\text{BR}(a \to \gamma\gamma)}{\text{BR}(a \to e\bar{e})} \approx \frac{(g_{a\gamma\gamma}^{\text{eff}})^2 m_a^2}{8(g_{a\bar{e}e}^{\text{eff}})^2 m_e^2}$$

Favor for diphoton at $\mathcal{O}$ GeV, but dielectron could be comparable at lower mass (beam dump).

Yan Luo

Models

- KSVZ-like model

Introduce a global $U(1)_{\rm PQ}$ symmetry, and a heavy vector-like $\mathcal{Q}$ + complex singlet Φ

	$\mathcal{Q}_L$	$\mathcal{Q}_R$	Φ
$U(1)_Y$	Y	Y	0
$U(1)_{PQ}$	$+1$	-1	$+2$

$$\mathscr{L} \supset |\partial^\mu \Phi|^2 + i\bar{\mathcal{Q}} D_\mu \gamma^\mu \mathcal{Q}$$
$$-(y\bar{\mathcal{Q}}_L \mathcal{Q}_R \Phi + \mathrm{h.c.}) - V(\Phi)$$

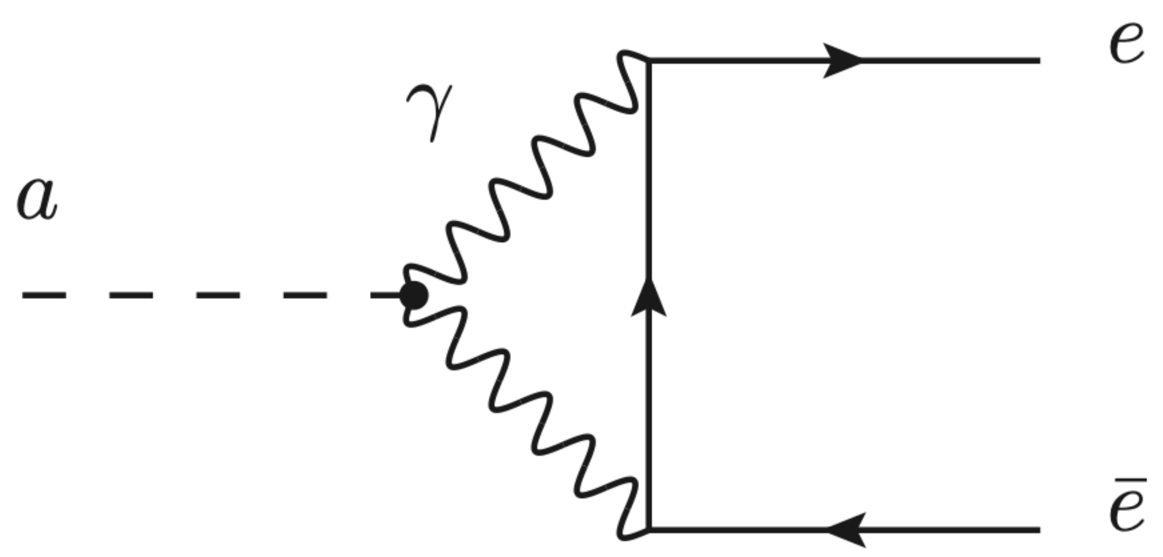

After symmetry breaking

$$\mathscr{L} \supset - m_{\mathcal{Q}} \bar{\mathcal{Q}}_L \mathcal{Q}_R e^{i\frac{a}{v_a}} + \mathrm{h.c.}$$

After chiral rotation

$$\delta\mathscr{L} = Y^2 \frac{\alpha_{\rm EM}}{4\pi} \frac{a}{v_a} F\tilde{F}$$

Loop contribution M. Bauer et al. 1708.00443

$$g_{a\bar{e}e}^{\rm eff} = g_{a\bar{e}e}^{0} + \frac{3\alpha_{\rm QED}}{4\pi} g_{a\gamma\gamma}^{\rm eff} \left[\ln\left(\frac{f_a^2}{m_e^2}\right) + g\left(\tau_e\right) \right]$$

$$g(\tau_e) = -\frac{1}{6}\left(\ln\left(\frac{m_a^2}{m_e^2}\right) - i\pi\right)^2 + \frac{2}{3} + \mathcal{O}\left(\frac{m_e^2}{m_a^2}\right) \qquad m_a^2 \gg m_e^2$$

Yan Luo

Models

- DFSZ-like model

Introduce a global $U(1)_{\mathrm{PQ}}$ symmetry, and
2HDM Φ_i + complex singlet S

$SU(2)_Y \times U(1)_Y \times U(1)_{PQ} \to U(1)_{EM}$ + two pseudoscalar G

the Yukawa terms

$$\mathscr{L} \supset -\bar{L}_L Y_d H_1 e_R + \mathrm{h.c.} = -ic_e \frac{a}{f_a}\bar{e} m_e \gamma_5 e$$

After chiral rotation, due to axial anomaly

$$\mathscr{L} \supset \frac{c_e}{2}\frac{\partial_\mu a}{f_a}\bar{e}\gamma^\mu\gamma_5 e - \frac{e^2}{16\pi^2}\frac{a}{f_a}F_{\mu\nu}\tilde{F}^{\mu\nu}$$

	Φ_1	Φ_2	S
$U(1)_Y$	$+1/2$	$+1/2$	0
$U(1)_{PQ}$	-1	$+1$	$+2$

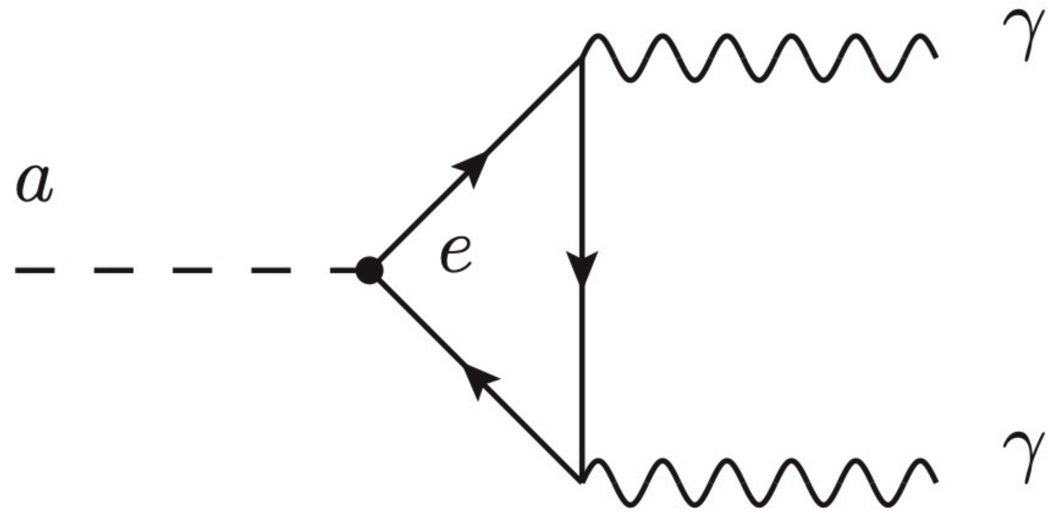

Loop contribution M. Bauer et al. 1708.00443

$$g_{\gamma\gamma}^{\mathrm{eff}} = \frac{e^2}{16\pi^2}\frac{1}{f_a}\sum_e (B_1(\tau_e)-1)c_e$$

$$B_1(\tau) = 1 - \tau f^2(\tau)$$

$$\tau_i = 4m_i^2/4m_a^2$$

$$f(\tau) = \begin{cases} \arcsin\dfrac{1}{\sqrt{\tau}} & \tau \geq 1 \\ \dfrac{\pi}{2} + \dfrac{i}{2}\ln\dfrac{1+\sqrt{1-\tau}}{1-\sqrt{1-\tau}} & \tau < 1 \end{cases}$$

Yan Luo

Models Interpretation

KSVZ-like

$$\frac{|g_{a\gamma\gamma}^{\rm eff}|}{|g_{a\bar{e}e}^{\rm eff}|} = \frac{8\pi}{\alpha_{\rm QED}\left|\left(6\ln\left(\frac{f_a^2}{m_e^2}\right) - \left(\ln\left(\frac{m_a^2}{m_e^2}\right) - i\pi\right)^2 + 4\right)\right|}$$

DFSZ-like

$$\frac{g_{a\gamma\gamma}^{\rm eff}}{g_{a\bar{e}e}^{\rm eff}} = \frac{\sum_{\ell=e,\mu,\tau}\left(B(\tau_\ell)-1\right)\frac{N_c Q_f^2 e^2}{16\pi^2} g_{a\bar{\ell}\ell}^{\rm eff}}{g_{a\bar{e}e}^{\rm eff}}$$

KSVZ-like favors for ALP-photon coupling, while DFSZ-like favors for ALP-lepton/electron coupling

J. Liu, **YL** and M. Song. 2304.05435

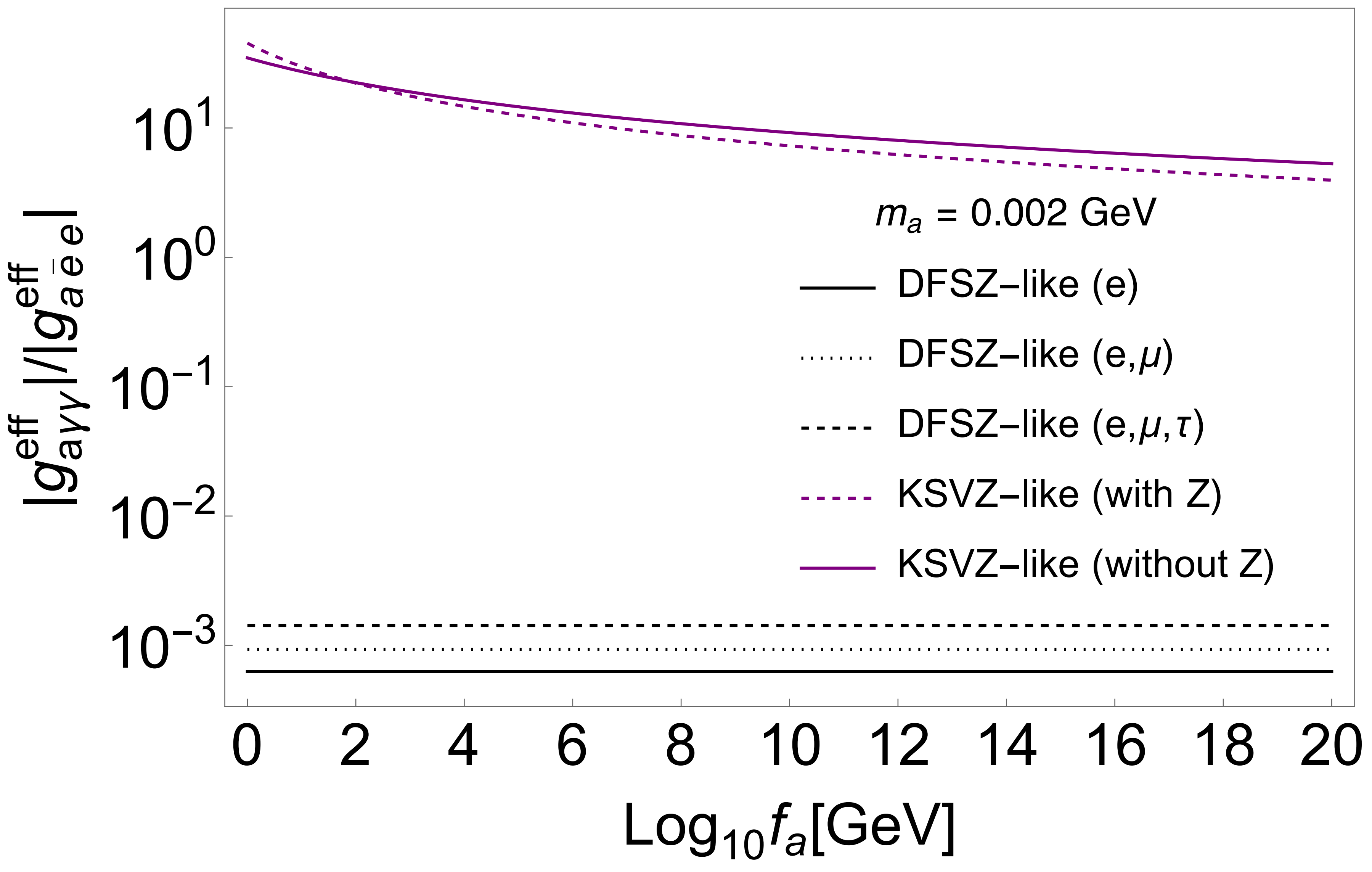

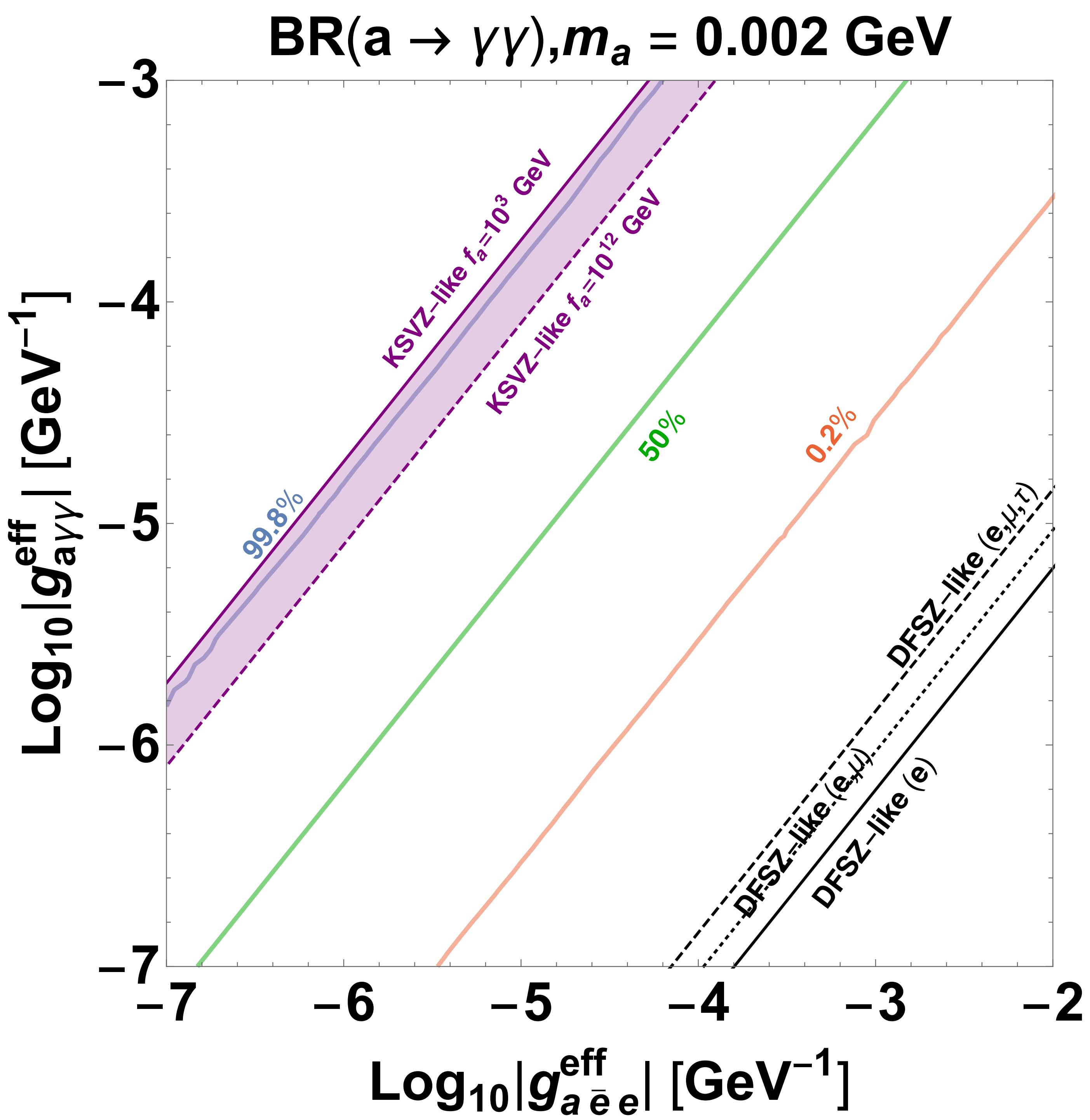

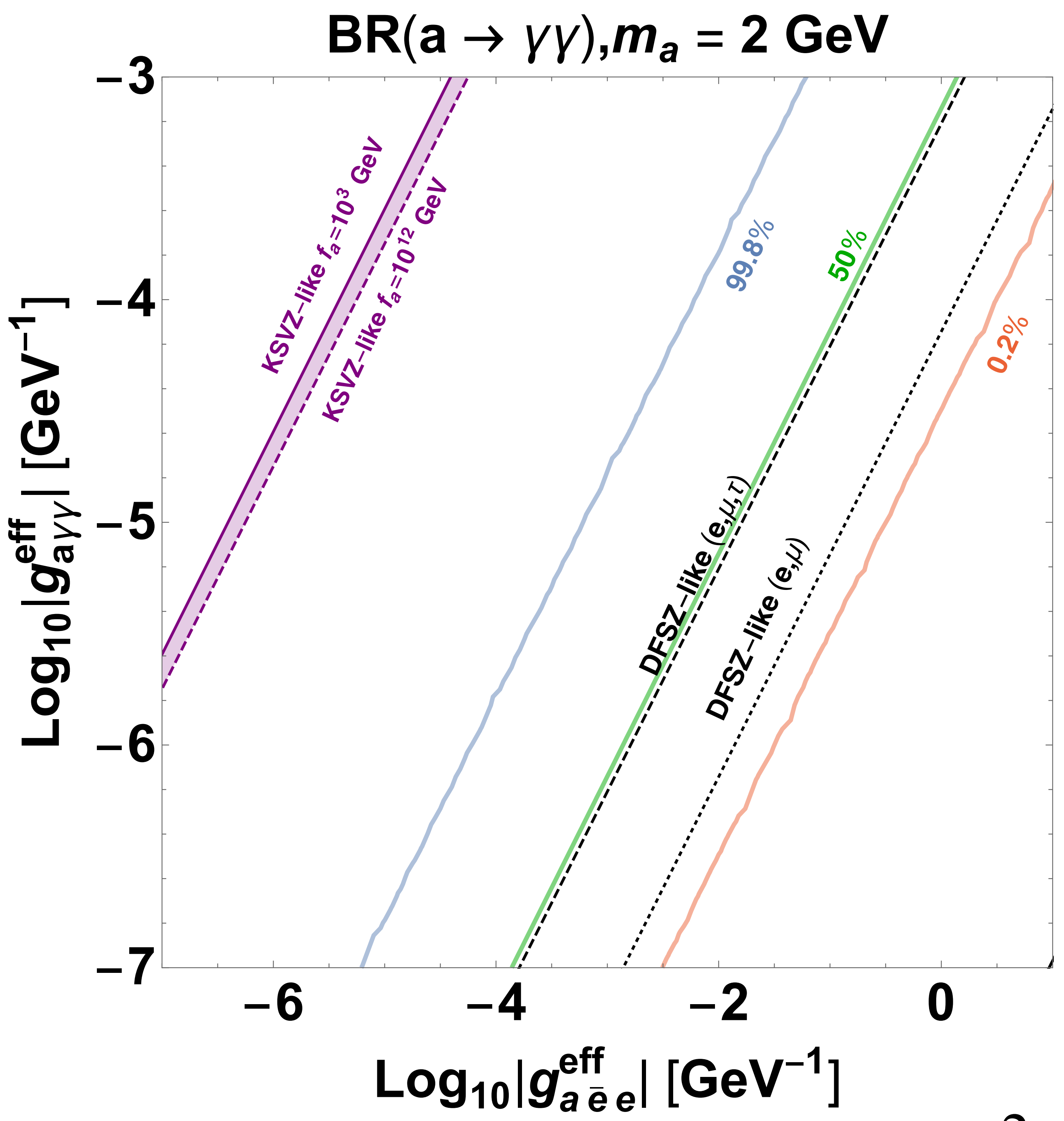

BR($a \to e^+e^-$) increase when m_a decrease due to m_a^2/m_e^2

Collider and Beam dump Experiments

- For $m_a \sim 0.1 - 10$ GeV, we focus on two electron collider experiments

  ($e^+ + e^- \to a + \gamma$ follows $a \to e^+e^-/\gamma\gamma$)

  Babar (Dark photon search) limits $g_{aee}^{\rm eff}$, two electron + one photon

  Belle-II limits $g_{a\gamma\gamma}^{\rm eff}$, from three photon final state

- For $m_a \sim$ MeV - GeV, NA64 and E137 beam dump experiments are investigated

  ($e + \gamma \to e + a$)

  NA64 and E137 beam dump experiments,

  both two experiments have constrained $g_{aee}^{\rm eff}$ and $g_{a\gamma\gamma}^{\rm eff}$

The concurrence effects of two couplings have a greater impact on electron beam dump searches.

Yan Luo

Babar and Belle-II Results Reinterpret

Production:

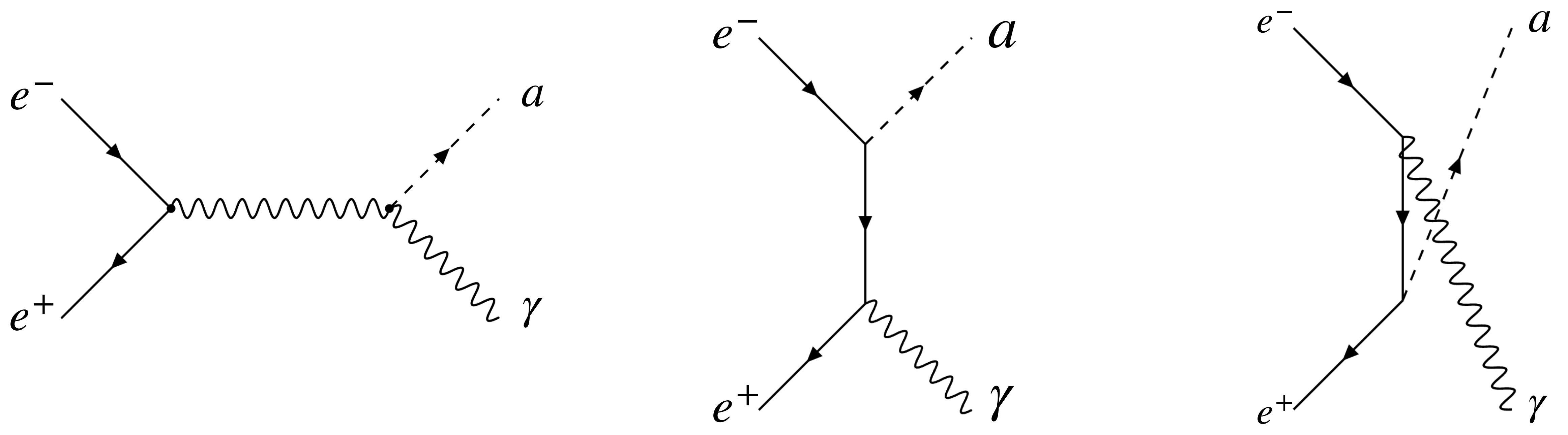

$$\sigma_{e^+e^-\to a\gamma} = \alpha_{\rm qed}\left[\frac{(g^{\rm eff}_{a\gamma\gamma})^2\left(s-m_a^2\right)^3}{24s^3} + m_e^2\left(\frac{(g^{\rm eff}_{a\gamma\gamma})^2\left(m_a^2-s\right)^4 + (3\ln 4)g^{\rm eff}_{a\gamma\gamma}g^{\rm eff}_{a\bar{e}e}s\left(m_a^2-s\right)^3}{6s^4\left(s-m_a^2\right)}\right)\right.$$
$$\left. + m_e^2\left(\frac{(3\ln 4)(g^{\rm eff}_{a\bar{e}e})^2 s^2\left(m_a^4+s^2\right)}{6s^4\left(s-m_a^2\right)}\right)\right] + \mathcal{O}(m_e^4)$$

the interference term is suppressed

- concurrence effect: σ and BR

$\sigma\uparrow$ as two couplings are incorporated (survived region squeezed)

BR $\downarrow$ when the other coupling is large (survived region relaxed)

J. Liu, **YL** and M. Song. 2304.05435

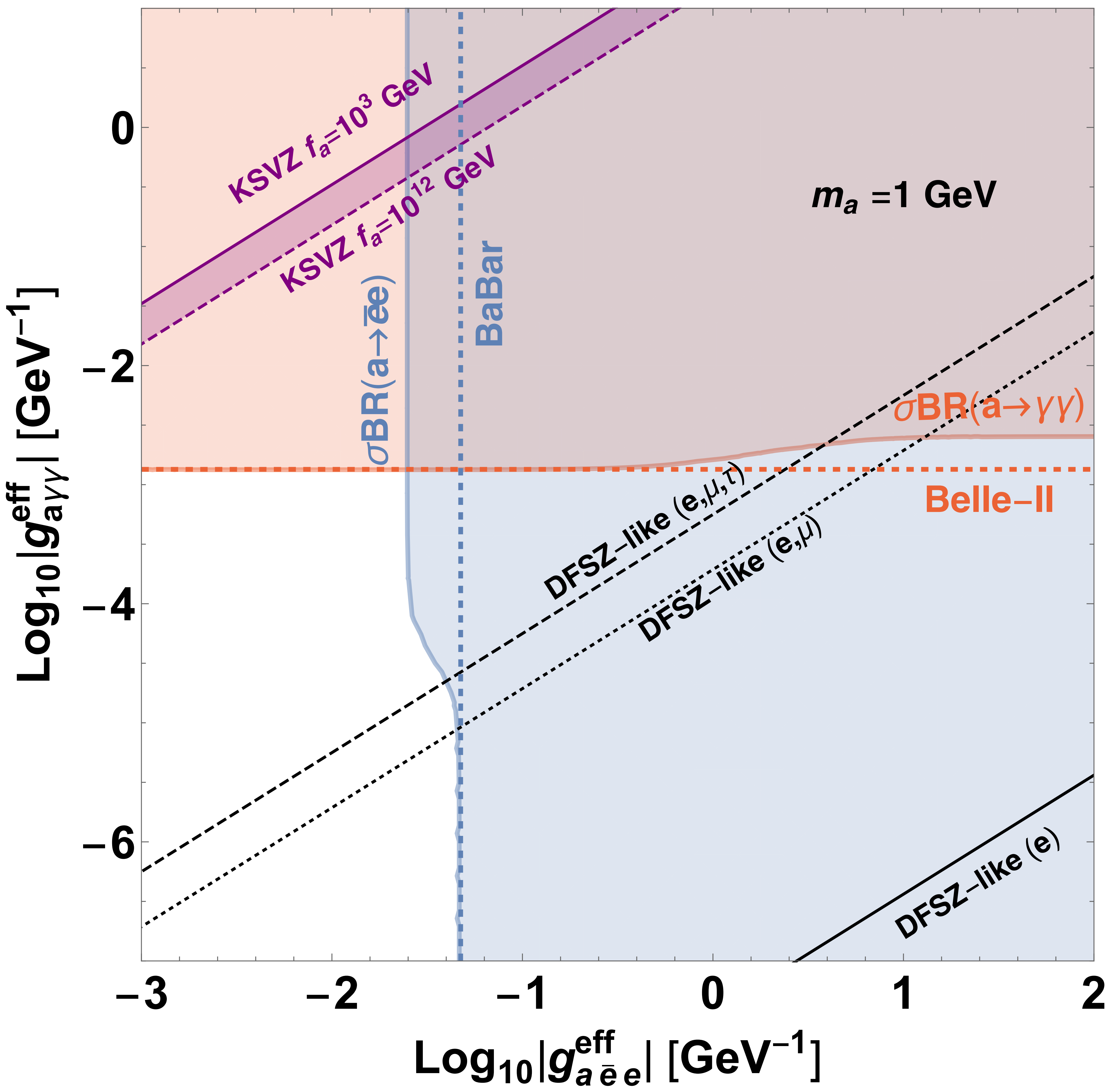

Horizontal(Belle-II) and vertical(BaBar) dashed lines are existing bounds (left bottom region is survived)

Yan Luo

Babar and Belle-II Results Reinterpret

J. Liu, **YL** and M. Song. 2304.05435

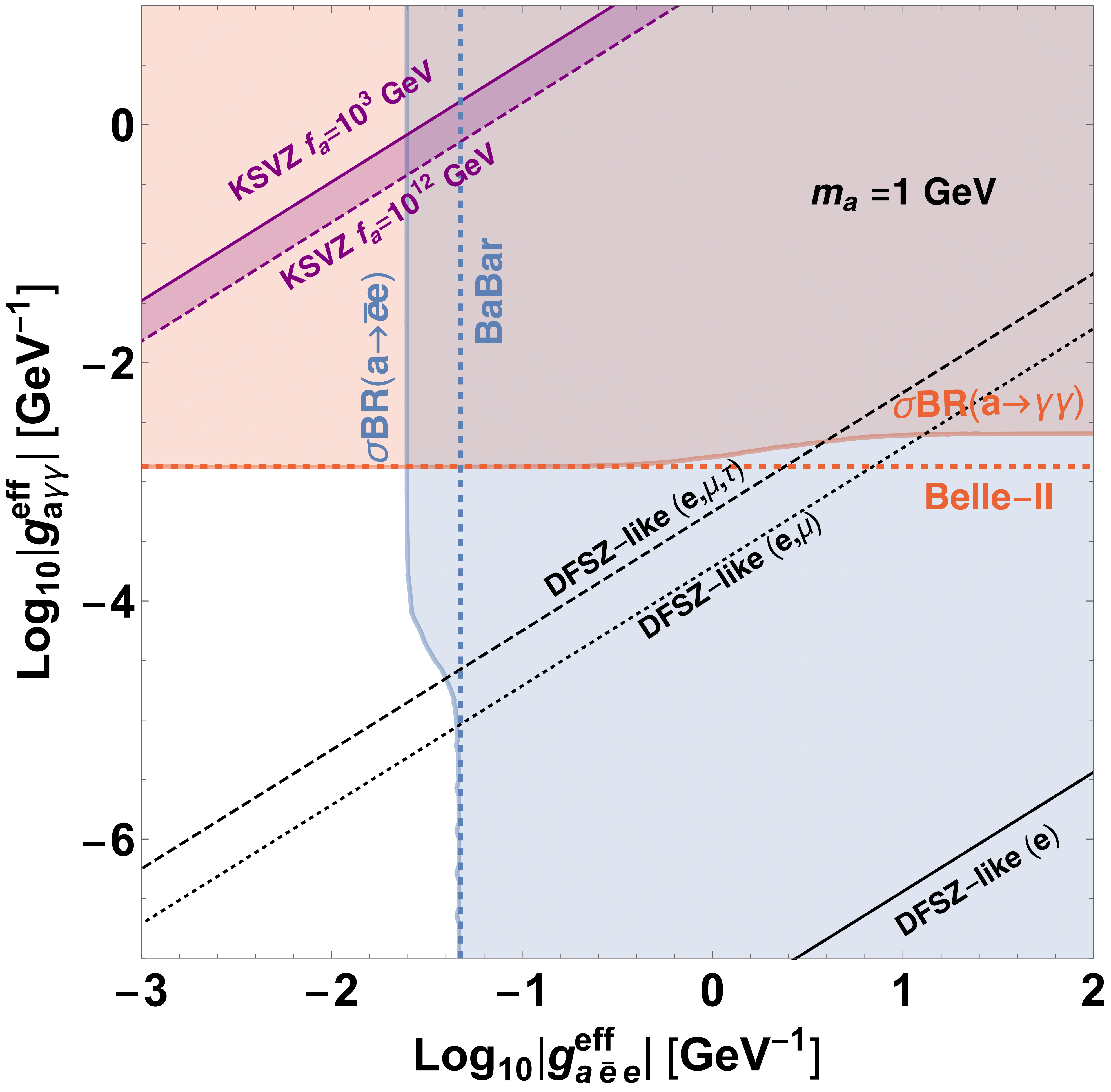

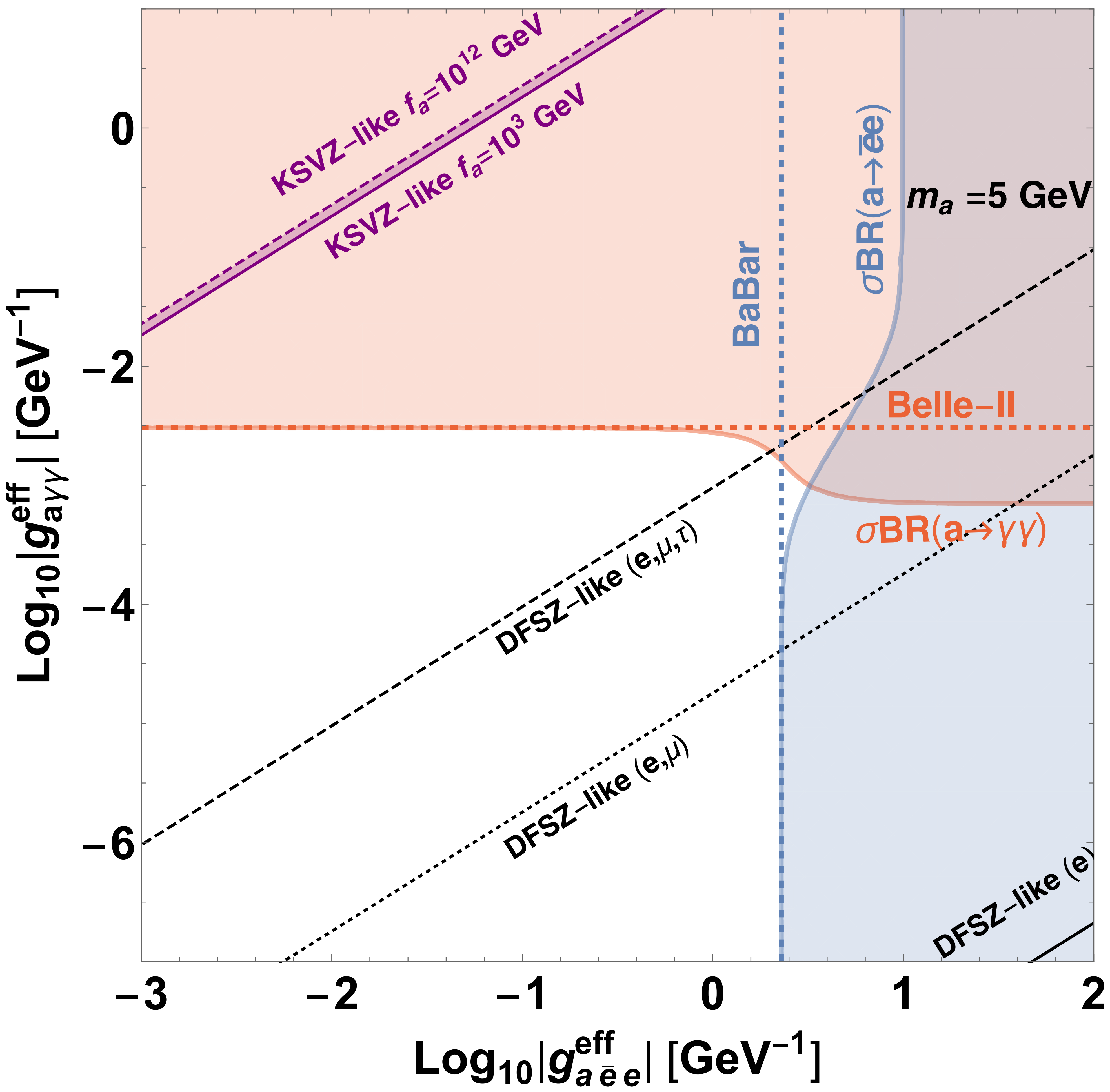

Yan Luo

E137 and NA64 Results Reinterpret

Production:

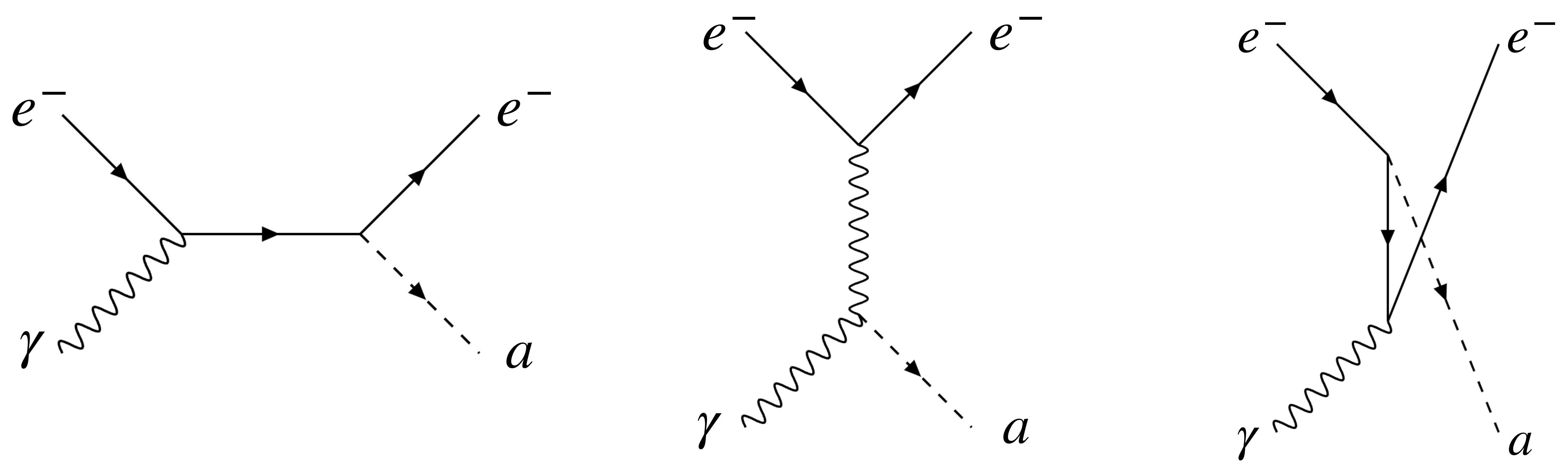

Improved Weizsäcker-Williams (IWW) approximation:

David McKeen et al. 1609.06781

$$\left(\frac{d\sigma}{dx}\right)_{IWW} = \frac{\alpha_{EM}}{4\pi^2}\frac{\sqrt{E^2x^2 - m_a^2}}{E}\chi\int d\tilde{u}\frac{\mathcal{A}_{2\to 2}}{\tilde{u}^2}\frac{1-x}{x}$$

reduce phase space integral $(2 \to 3 \Rightarrow 2 \to 2)$

$x = E_a/E_0$ fraction of energy

effective flux of photon:

$$\chi = \int_{t_{\min}}^{m_a^2+m_e^2}\frac{t - t_{\min}}{t}F^2(t)$$

the number of detectable ALP:

$$N_a \approx \frac{N_e X}{M_{target}}\int_{E_{min}}^{E_0} dE\int_{x_{min}}^{x_{max}} dx\int_0^T dt I_e(E_0, E, t)\frac{d\sigma}{dx}e^{-\frac{L_{\rm sh}}{l_a}}(1 - e^{-\frac{L_{\rm dec}}{l_a}}) \qquad l_a = \frac{E_a}{m_a}\frac{1}{\Gamma_a}$$

I_e: radiation loss function

Yan Luo

E137 and NA64 Results Reinterpret

Experiment	E_e[GeV]	Target	$L_{\rm sh}$[m]	$L_{\rm dec}$[m]	Year
E137	20	Al	179	204	1988(SLAC)
NA64(Invis)	100	Pb	$\sim$ 4.35	∞	2020(CERN)
KEK	7	W	$\sim$ 0.25	1	2013(KEK linac)
E141	9.0	W	0.12	35	1987(SLAC)
E774	275	W	0.3	28	1989(Fermilab)
Orsay(Higgs)	1.6	W	1	2	1989(LAL)

NA64 (Invis) represents the invisible signature configuration of NA64, where ALPs decay beyond all subdetectors of NA64.

Invisible: $L_{\rm sh}$ = one ECAL + three HCAL, and $L_{\rm dec} = \infty$

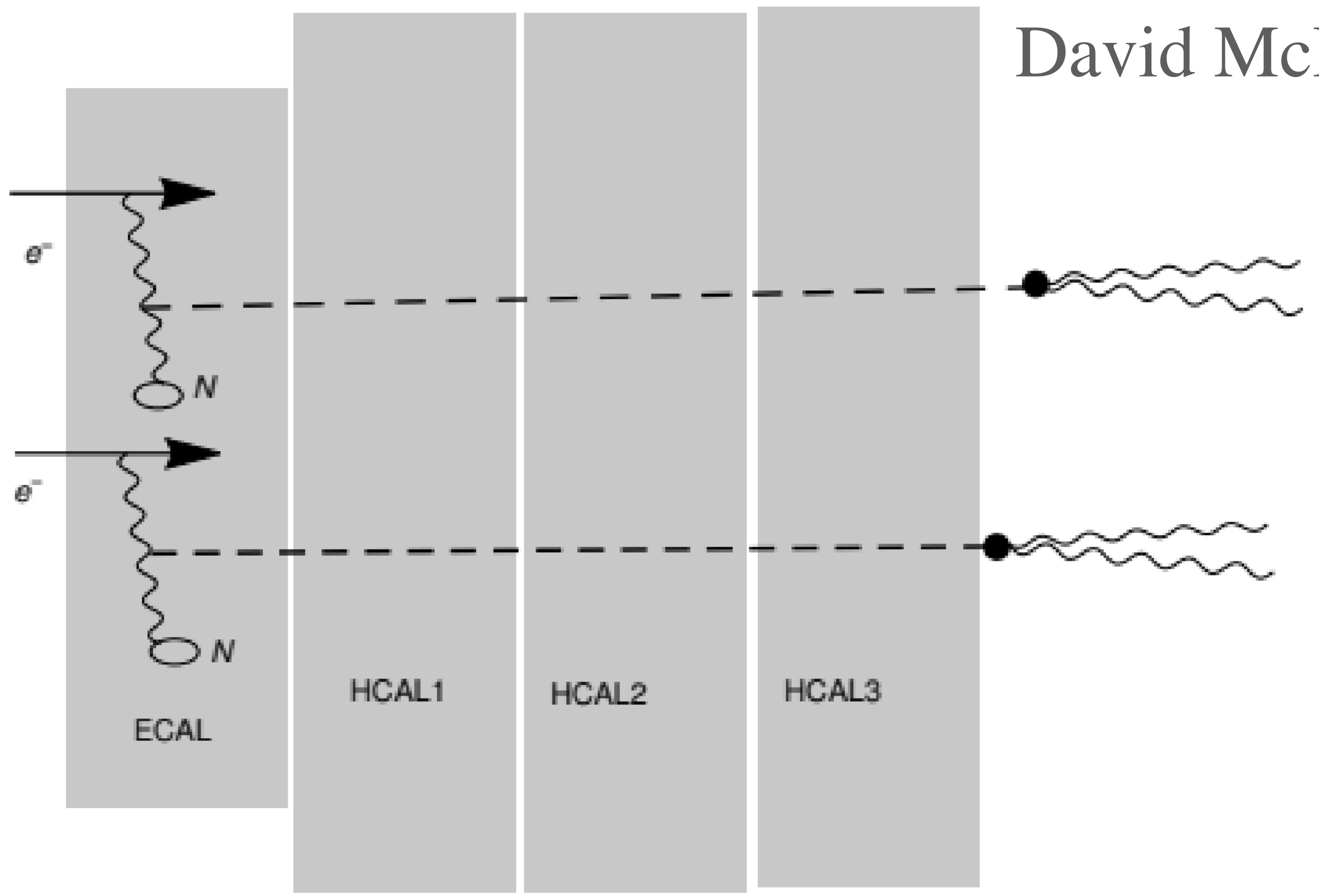

David McKeen et al. 1609.06781

Yan Luo

E137 and NA64 Results Reinterpret

J. Liu, **YL** and M. Song. 2304.05435

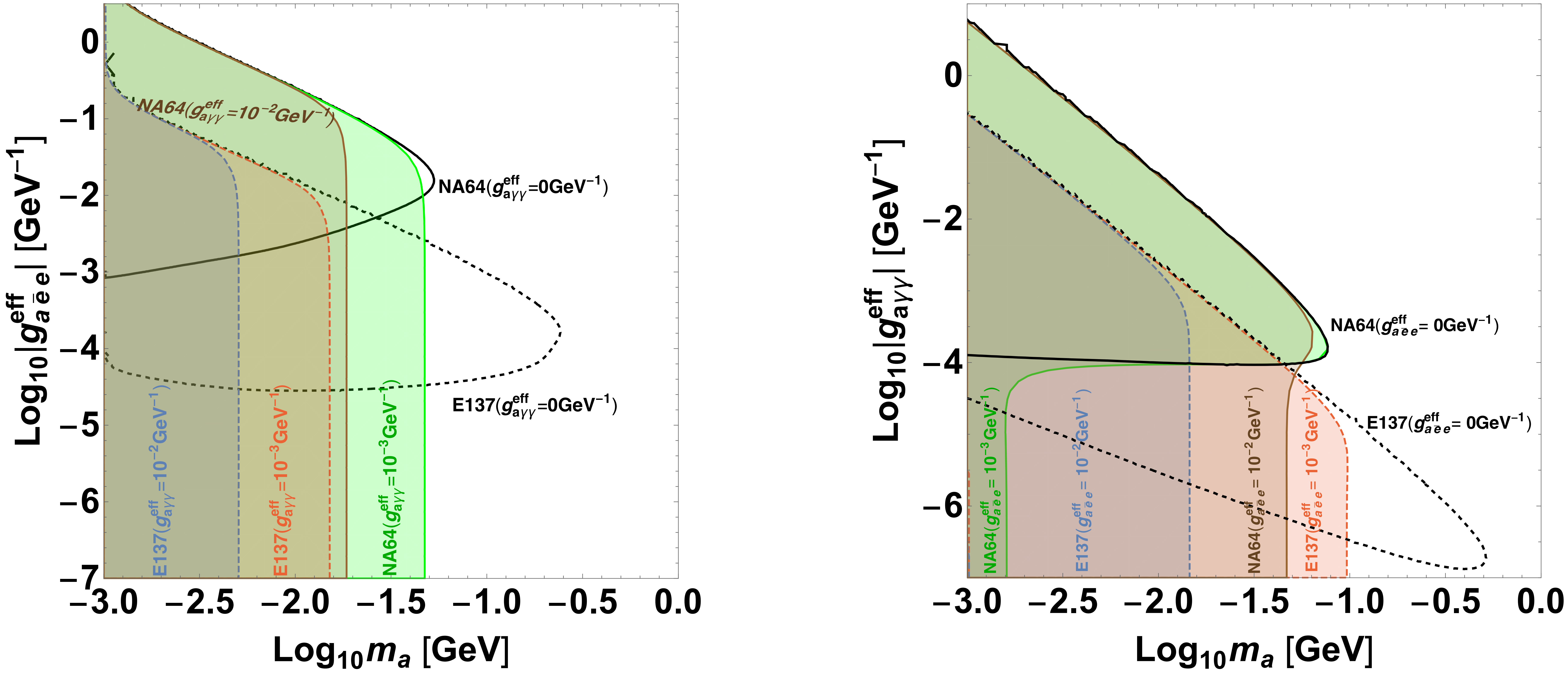

Solid line (NA64), dashed line (E137) are recent existing bounds (region inside excluded).

- concurrence effect: σ and τ_a

  $\Gamma_a \uparrow$ affects $l_a \downarrow$, so $N_a \downarrow$ in the large m_a coupling region
  $N_a \uparrow$ in the lower coupling region due to larger cross section, and hard to distinguish electron/photon in the final state

Constraints for DFSZ-like (e) Model

J. Liu, **YL** and M. Song. 2304.05435

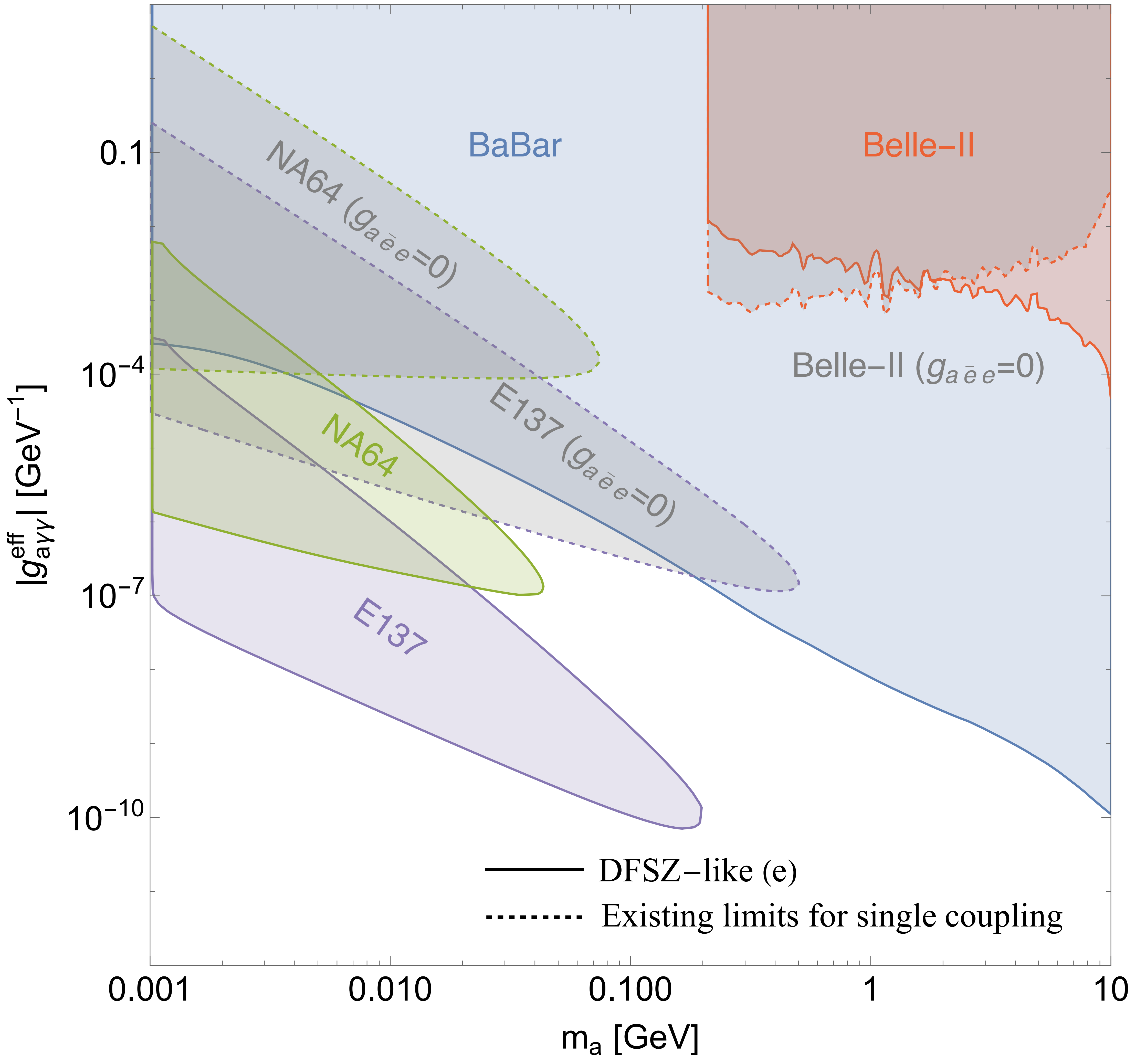

- Babar constraints are indirectly derived from $g_{a\bar{e}e}^{\rm eff}$
- downward shift for beam dump constraints

Conclusion

- The axion ULDM can be searched through radio telescope, by looking for the photon signal converted from axion.
- We used the observation data from LOFAR to search for resonantly converted mono-chromatic EM waves from ULDM in solar corona. We delt with data processing and handled the complexity of plasma environment, constraining the ULDM axion or dark photon.
- For massive axion, existing limits usually consider individual coupling, while multi-coupling emerge naturally from radiative corrections and may play an role.
- We investigate the collider and beam dump experiments, and the precent limits will be modified in concurrence scenario, significantly for beam dump experiments.

Backup

Check: Small-scale Fluctuations

- Plasma density fluctuations

$$P_{a\to\gamma}(v_{rc}) = \pi \frac{g_{a\gamma\gamma}^2 \left|\mathbf{B}_T\right|^2}{m_a} v_{rc}^{-1} \left| \frac{\partial \ln \omega_p^2(r)}{\partial r} \right|_{r=r_c}^{-1}$$

may influence the application of approximation
may modify the conversion probability, by altering $\nabla \omega_p$

model the density fluctuations through the spatial power spectrum

$$C(\mathbf{d}) \equiv \left\langle \delta n_e(\mathbf{x}) \delta n_e(\mathbf{x}+\mathbf{d}) \right\rangle \qquad C(\mathbf{d}) = \int_{-\infty}^{\infty} e^{-i\mathbf{q}\cdot\mathbf{d}} P(q) d^3\mathbf{q}$$

$P(q) = C_n q^{-\alpha}$ Kolmogorov spectrum: $\alpha = 11/3$

G. Thejappa et al. The Astrophysical Journal, Volume 676, Issue 2, pp. 1338-1345 (2008)

- Check WKB and saddle point approximation

$$\delta l_e \simeq \left| \frac{n_e'}{n_e} \right|^{-1} \simeq \left[\frac{\alpha-3}{5-\alpha} \epsilon_e^2 q_o^{\alpha-3} q_i^{5-\alpha} \right]^{-\frac{1}{2}} \approx 10^{-3} q_o^{-1}$$

WKB requirement: $\delta l_e k_{A'} \approx 30 \gg 1$

$$F(r) \equiv \int^r \frac{\omega_p^2(r') - m_{A'}^2}{2k_{A'}} dr'$$

$$\frac{\frac{1}{2!}F''(r)}{\frac{1}{3!}\delta l_{\rm res} F'''(r)} \simeq \frac{3}{\sqrt{2\pi}} \frac{[F''(r)]^{3/2}}{F'''(r)} = 3\sqrt{\frac{\alpha_{\rm EM}\epsilon_e n_e}{k_{A'} m_e}} \left(\frac{(\alpha-3)(7-\alpha)^2}{(5-\alpha)^3} q_o^{\alpha-3} q_i^{1-\alpha} \right)^{\frac{1}{4}} \approx 5$$

$$P_{A'\to\gamma} = \left| \int_{r_0}^{r} dr' \frac{-\epsilon m_a^2}{2k_r} e^{i\int_{r_0}^{r'} dr'' \frac{1}{2k_r}\left[\omega_p(r'')^2 - m_a^2\right]} \right|^2 .$$

fluctuation scale $l_i = \frac{684}{\sqrt{n_e/\text{cm}^{-3}}} \sim 0.1$ km, $l_o \sim 10^6 l_i$ $\qquad q = \frac{2\pi}{l}$

Check: Small-scale Fluctuations

Check the conversion probability

modeled in discrete Fourier modes:

$$n_e(r) = \frac{r_c^2}{r^2}\left(n_{e,\mathrm{bkg}}(r_c) + \sum_{n=0}^{N} \delta n_e(q_n)\Delta \cdot \sin\left[q_n(r-r_c)+\phi_n\right]\right)$$

may change the conversion probability, explore **numarically**:

$$r_{\mathrm{dn}} = \frac{\sum_{n_e(r')=n_e(r_c)} \left| \frac{1}{n_e(r)}\frac{dn_e(r)}{dr}\right|^{-1}_{r=r'}}{\left| \frac{1}{n_{e,\mathrm{bkg}}(r)}\frac{dn_{e,\mathrm{bkg}}(r)}{dr}\right|^{-1}_{r=r_c}}$$

Increasing resonant points, but **decreasing** conversion probability for each points.
Numerical simulation: fluctuation has **minimal** impact.

H. An, X. Chen, S. Ge, J. Liu and **YL**. 2301.03622